 doi:10.20944/preprints202012.0252.v1

Unforgettable: optogenetic stimulation of prelimbic pyramidal neurons maintains fear memories by modulating amygdala pyramidal neuron transcriptome

Laricchiuta Daniela[1], Sciamanna Giuseppe[1], Gimenez Juliette[1], Termine Andrea[1,2], Fabrizio Carlo[1,2], Caioli Silvia[3], Balsamo Francesca[1], Panuccio Anna[1,4], De Bardi Marco[1], Saba Luana[1], Passarello Noemi[1], Cutuli Debora[1,4], Mattioni Anna[1], Zona Cristina[2], Orlando Valerio[1,5] and Petrosini Laura[1]

[1] IRCCS Fondazione Santa Lucia, 00143 Rome, Italy

[2] Department of Systems Medicine, Tor Vergata University of Rome, 00133 Rome, Italy

[3] Unit of Neurology, IRCCS Neuromed, 86077 Pozzilli (Is), Italy

[4] Department of Psychology, University "Sapienza" of Rome, 00185 Rome, Italy

[5] King Abdullah University of Science and Technology (KAUST), Biological Environmental Science and Engineering Division, KAUST Environmental Epigenetics Program, 23955-6900 Thuwal, Saudi Arabia

Corresponding author:

Daniela Laricchiuta

E-mail: daniela.laricchiuta@gmail.com

 doi:10.20944/preprints202012.0252.v1

Abstract

Fear extinction requires coordinated neural activity within the amygdala and medial prefrontal cortex (mPFC). Any behavior has a transcriptomic signature that is modified by environmental experiences, and specific genes are involved in functional plasticity and synaptic wiring during fear extinction. Here, we investigated the effects of optogenetic manipulations of prelimbic (PrL) pyramidal neurons on amygdala gene expression to analyze the specific transcriptional pathways involved in adaptive and maladaptive fear extinction. To this aim, transgenic mice were (or not) fear-conditioned and during the extinction phase they received optogenetic (or sham) stimulations over PrL pyramidal neurons. At the end of behavioral testing, electrophysiological (neural cellular excitability and Excitatory Post-Synaptic Currents) and morphological (spinogenesis) correlates were evaluated in the PrL pyramidal neurons. Furthermore, transcriptomic cell-specific RNA-analyses (differential gene expression profiling and functional enrichment analyses) were performed in amygdala pyramidal neurons. Our results show that the optogenetic activation of PrL pyramidal neurons in fear-conditioned mice induces fear extinction deficits, reflected in an increase of cellular excitability, excitatory neurotransmission, and spinogenesis of PrL pyramidal neurons, and in strong modifications of the transcriptome of amygdala pyramidal neurons. Understanding the electrophysiological, morphological and transcriptomic architecture of fear extinction may facilitate the comprehension of fear-related disorders.

Keywords

Fear extinction; Fear Conditioning; Medial Prefrontal Cortex; RNA sequencing; Differential Gene Expression; Electrophysiological Recordings; Excitatory Post-Synaptic Currents; Spinogenesis; Fear-related Disorders.

 doi:10.20944/preprints202012.0252.v1

1. Introduction

In variable and challenging environments with various contextual situations, the individuals face a number of approaching dangers. The knowledge of potential threats allows developing fear of threatening situations, choosing among the various behaviors the safest ones, and detecting future dangers. To develop adaptive fear responses, the brain has to discriminate different sensory cues and associate relevant stimuli with aversive events [1]. Thus, when a relevant stimulus (or a context) is associated with an aversive event, the fear associative learning and memory take place.

Learned fear has been widely studied using Classical Fear Conditioning (CFC), a very useful paradigm to analyze the neuronal and molecular bases of fear associative learning and memory [2,3]. In experimental models in which the CFC paradigm is implemented, the conditioned stimulus (CS), such as a specific cue or context, is associated with the unconditioned stimulus (US), such as foot-shock [3,4]. After the association has taken place, CS alone is able to induce the conditioned response (CR) of fear, such as freezing behavior. Interestingly, the CR to CS is gradually weakened by repeated exposure to unreinforced (presented without US) CS. In fact, the extinction of fear memory when the danger is gone is so crucial to implement other survival functions that the impairment of the coping mechanisms dampening fear memory results in maladaptive behaviors. Extinguishing a fear response does not simply involve the fading away of the previous learning. Rather, during extinction process the subject learns something new - the cue no longer predicts that the fearful event will occur [5]. Compromised fear extinction is the key clinical feature of several fear-related disorders, such as post-traumatic stress disorders (PTSD), generalized anxiety, major depression, and phobias [5]. The acquisition of CS-US associative memory and the acquisition and maintenance of extinction memory require coordinated neural activity within the amygdala, medial prefrontal cortex (mPFC), and hippocampus [6–11]. Specifically, the activation of pyramidal neurons of the baso-lateral amygdala (BLA) is necessary to associate sensory input with fear CR [12,13]. Interacting with the amygdala, the mPFC combines information from multiple inputs to exert top-down control allowing for appropriate responses. In this framework, it has been demonstrated that the balance between expression and extinction of fear CR is modulated by inputs from/to the amygdala to/from two sub-regions of the mPFC: the prelimbic cortex (PrL), which promotes fear responses, and the infralimbic cortex (IL), which promotes fear extinction [14,15].

 doi:10.20944/preprints202012.0252.v1

To test the activation or deactivation of the BLA-mPFC network in transmitting learned fear CS-US association, *in vivo* optogenetic manipulations were performed by stimulating or inhibiting, with advanced spatial and temporal precision, specific neurons in the brain areas involved in fear processing [14,16–20]. Fear extinction decreases the efficacy of excitatory synaptic transmission in the projections from mPFC to BLA, whereas inhibitory responses are not altered [21]. In parallel, projections from BLA to PrL exhibit cell-type-specific plasticity during states of high fear, whereas projections from BLA to IL are recruited during states of low fear [19]. Thus, *in vivo* optogenetics allows understanding the causal relationships between neuronal firing and behavior.

It has to be noted that any behavior has a specific genomic, transcriptomic, and epigenetic signature. Namely, transcriptomic changes are a crucial component of the neuronal modifications that underlie learning and memory [22–24], also after the fear exposure [25–27]. To date, specific genes involved in functional plasticity and synaptic wiring during fear memory are retained possible disease contributors and potential therapeutic targets for fear-related disorders [28–32]. The environmental experiences may modify the transcriptome [33–36], and these modifications, in turn, may explain the variability in resilience or predisposition to fear-related disorders as well as the severity of their symptomatology [37]. Understanding the transcriptomic architecture of compromised fear inhibition may thus facilitate the comprehension of fear-related disorders and the identification of potential therapeutic targets.

In the present study, adult mice were submitted to CFC receiving (or not) the US, to test the synergy between the activity of the amygdala and mPFC in fear learning. *In vivo* optogenetic manipulations were delivered to maintain the US-related activation of the PrL pyramidal neurons and impair fear extinction. At the end of behavioral testing, electrophysiological, morphological, and transcriptomic correlates were evaluated. Namely, in PrL pyramidal neurons neural cellular excitability and excitatory neurotransmission as well as spinogenesis were evaluated. In parallel, amygdala pyramidal neurons were sorted to perform cell-specific RNA-analyses (differential gene expression profiling and functional enrichment analysis). These analyses permitted us to drive a genome-wide investigation of pyramidal neuron expression patterns without *a priori* selection of specific gene factors, thus preventing bias in gene expression brought by bulk tissue analysis and biological subject pooling. Notably, investigating the effects of mPFC optogenetic manipulations on amygdala pyramidal neurons gene expression revealed specific transcriptional pathways involved in impaired fear extinction.

Preprints (www.preprints.org) | NOT PEER-REVIEWED | Posted: 10 December 2020 doi:10.20944/preprints202012.0252.v1

2. Results

2.1 Behavioral results: in vivo optogenetics of the PrL pyramidal neurons during contextual FC

The animals were (or not) fear-conditioned by using the CFC with repetitive sessions on day 1 (Conditioning phase), and 2, 3, 4, 7, and 14 (Extinction phase) (Figure 1A). During the extinction phase, the mice received optogenetic (OPTO FEAR and OPTO NOT FEAR groups) or sham (SHAM FEAR and SHAM NOT FEAR groups) stimulations. A three-way ANOVA (stimulation x fear x day) on freezing behavior (measured during 0-3 min of CFC) (Figure 1B) revealed significant stimulation ($F_{1,36}$=6.13; P=0.018), fear ($F_{1,36}$=63.29; P<0.0001), and day ($F_{5,36}$=50.27; P<0.0001) effects. The first-order interactions (at least P=0.05), as well as the second-order interaction (stimulation x fear x day) ($F_{5,180}$=3.00; P=0.013) were significant. As revealed by Newman-Keuls post-hoc comparisons, while all animals showed similar responses in the 0-3 min of Conditioning phase, only the fear-conditioned animals (OPTO FEAR and SHAM FEAR groups) showed consolidation processes of aversive memories on day 2, as revealed by their significantly increased freezing times between the Conditioning phase and day 2 (P=0.00004 for both OPTO FEAR and SHAM FEAR groups), and by the similar freezing times of the two groups (P=0.90). As expected, SHAM FEAR animals progressively extinguished fear memories over time and on day 14 their freezing behavior returned to a level similar (P=0.17) to that showed during the Conditioning phase. Interestingly, no extinction of fear memories was observed in OPTO FEAR group. On day 14, OPTO FEAR mice still displayed freezing times significantly longer than those of the Conditioning phase (P=0.00002). One-way ANOVA on freezing behavior (measured during 0-6 min of day 14) of all groups revealed a significant group effect ($F_{3,36}$=11.05; P=0.00003) (Figure 1C). As revealed by Newman-Keuls post-hoc comparisons, OPTO FEAR group showed the highest freezing times in comparison to the remaining groups (at least P=0.0005).

Preprints (www.preprints.org) | NOT PEER-REVIEWED | Posted: 10 December 2020 doi:10.20944/preprints202012.0252.v1

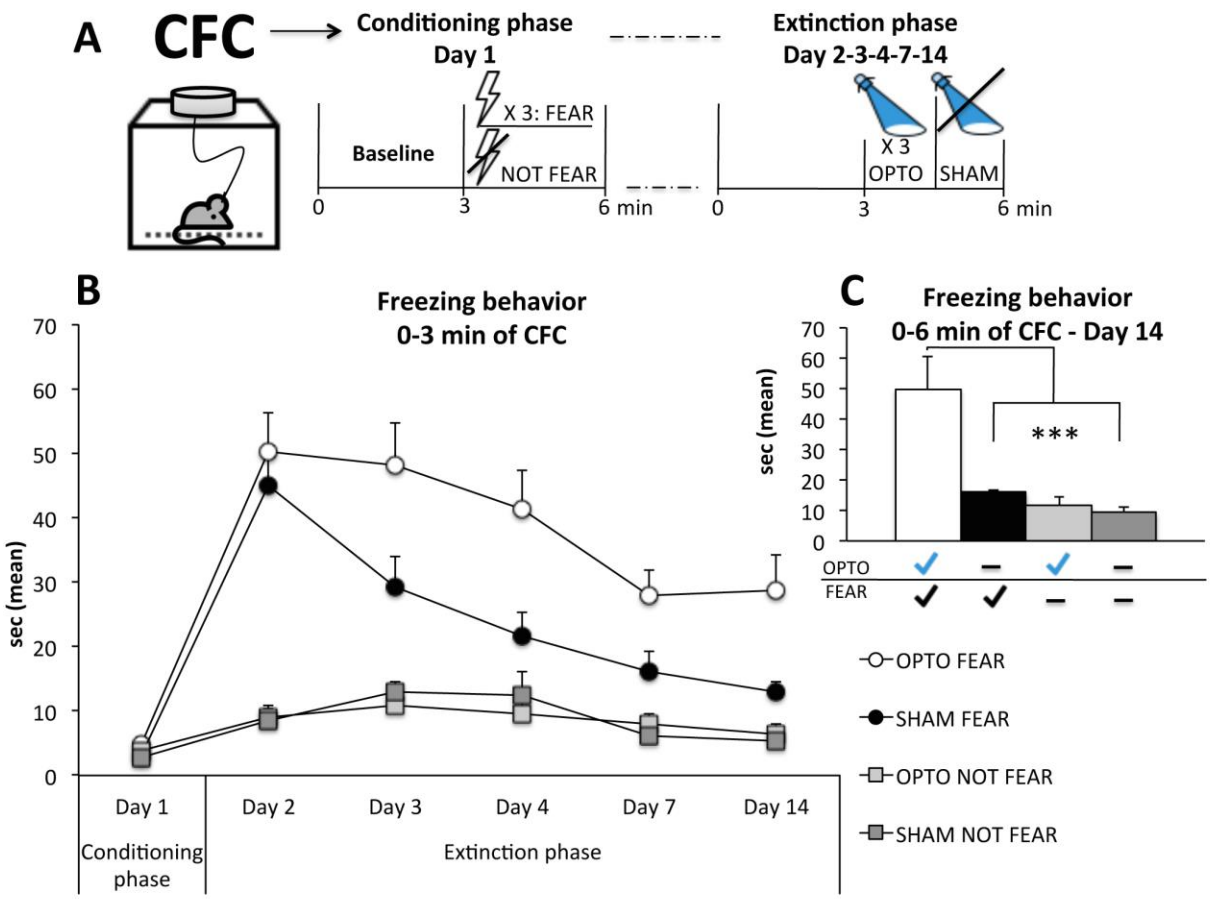

Figure 1. Experimental procedures and behavioral results of *in vivo* optogenetics of the PreLimbic (PrL) pyramidal neurons during Contextual Fear Conditioning (CFC). A) On day 1 (Conditioning phase) of CFC, each Thy1-COP4 mouse was allowed to explore the conditioning chamber for 3 min (Baseline). Afterward, half of the entire sample received three foot-shocks. On days 2, 3, 4, 7, and 14 (Extinction phase), the fear-conditioned and not fear-conditioned mice were placed again in the conditioning chamber for 6 min. During the Extinction phase, no shock was delivered and the mice received three optogenetic or sham stimulations of PrL pyramidal neurons. B) Freezing behavior measured during 0-3 min of CFC. All animals showed similar responses in the Conditioning phase and only the fear-conditioned animals (OPTO FEAR and SHAM FEAR groups) showed increased freezing times on day 2. While SHAM FEAR group progressively extinguished fear memories over time, no extinction of fear memories was observed in OPTO FEAR group. C) Freezing times measured during 0-6 min of day 14. OPTO FEAR group showed the highest freezing times in comparison to the remaining groups (*** P=0.0005).

Preprints (www.preprints.org) | NOT PEER-REVIEWED | Posted: 10 December 2020 doi:10.20944/preprints202012.0252.v1

2.2 Electrophysiological results: Cellular excitability of PrL pyramidal neurons

To test the ability of the optogenetics to modulate the activity of PrL cortex in fear-conditioned or not fear-conditioned animals, an extensive characterization of the cellular excitability of pyramidal layer 5 neurons after sham or optogenetic stimulation was performed.

In OPTO FEAR group, the optogenetic stimulation induced a robust increase in the evoked firing activities triggered by growing pulses of depolarizing current (0 to 400 pA). Neurons of OPTO FEAR animals clearly showed a higher number of action potentials in comparison to neurons of SHAM FEAR animals, at all current levels considered as indicated by cumulative curve (Correlation test, SHAM FEAR group: Pearson r=0.99, R^2=0.99; OPTO FEAR group: Pearson r=0.98, R^2=0.97; P<0.0001, Figure 2A). Rheobase that represents the lowest current amplitude able to generate an action potential is a further useful parameter to investigate changes in neural excitability. PrL pyramidal neurons of OPTO FEAR group recorded after optogenetic stimulation showed a clear reduction in the rheobase value in comparison to neurons of SHAM FEAR group (SHAM FEAR group: 69.88±5.5 pA, OPTO FEAR group: 50.50±3.7 pA, Mann-Whitney U Test P=0.002; Figure 2B). To test the effect of optogenetic stimulation upon glutamatergic input to pyramidal neurons, the Excitatory Post-Synaptic Currents (EPSC) have been recorded in OPTO FEAR and SHAM FEAR groups. To avoid any inhibitory current contamination, the recordings have been made under pharmacological isolation by bath application of the GABAA blocker, Picrotoxin (10 min, 50µM). Pyramidal PrL neurons of OPTO FEAR group showed a significantly higher frequency with respect to neurons of SHAM FEAR group (SHAM FEAR group: 4.11±0.26 Hz, OPTO FEAR group: 6.01±0.25 Hz, Mann-Whitney U Test P=0.002, Figure 2C). Cumulative plot clearly corroborated such an effect (Correlation test, SHAM FEAR group: Pearson r=0.85, R^2=0.72; OPTO FEAR group: Pearson r=0.75, R^2=0.56, P=0.0004, Figure 2C). No significant differences in EPSC amplitudes were found between SHAM FEAR and OPTO FEAR groups (SHAM FEAR group: 17.24±0.81 pA; OPTO FEAR group: 18.31±0.69 pA, Mann-Whitney U Test P= 0.37, data not shown).

Conversely, in both groups of not fear-conditioned animals (SHAM NOT FEAR and OPTO NOT FEAR groups) the optogenetic stimulation did not produce any significant difference in cellular excitability. Neither the evoked firing nor the rheobase nor EPSC frequency showed any significant difference between SHAM NOT FEAR and OPTO NOT FEAR groups (Figure 2D).

Preprints (www.preprints.org) | NOT PEER-REVIEWED | Posted: 10 December 2020 doi:10.20944/preprints202012.0252.v1

Taken together these data demonstrate that optogenetic stimulation was able to modify the intrinsic cellular excitability of PrL pyramidal neurons supporting the assumption that this area is involved in modulation of the fear responses during extinction phase.

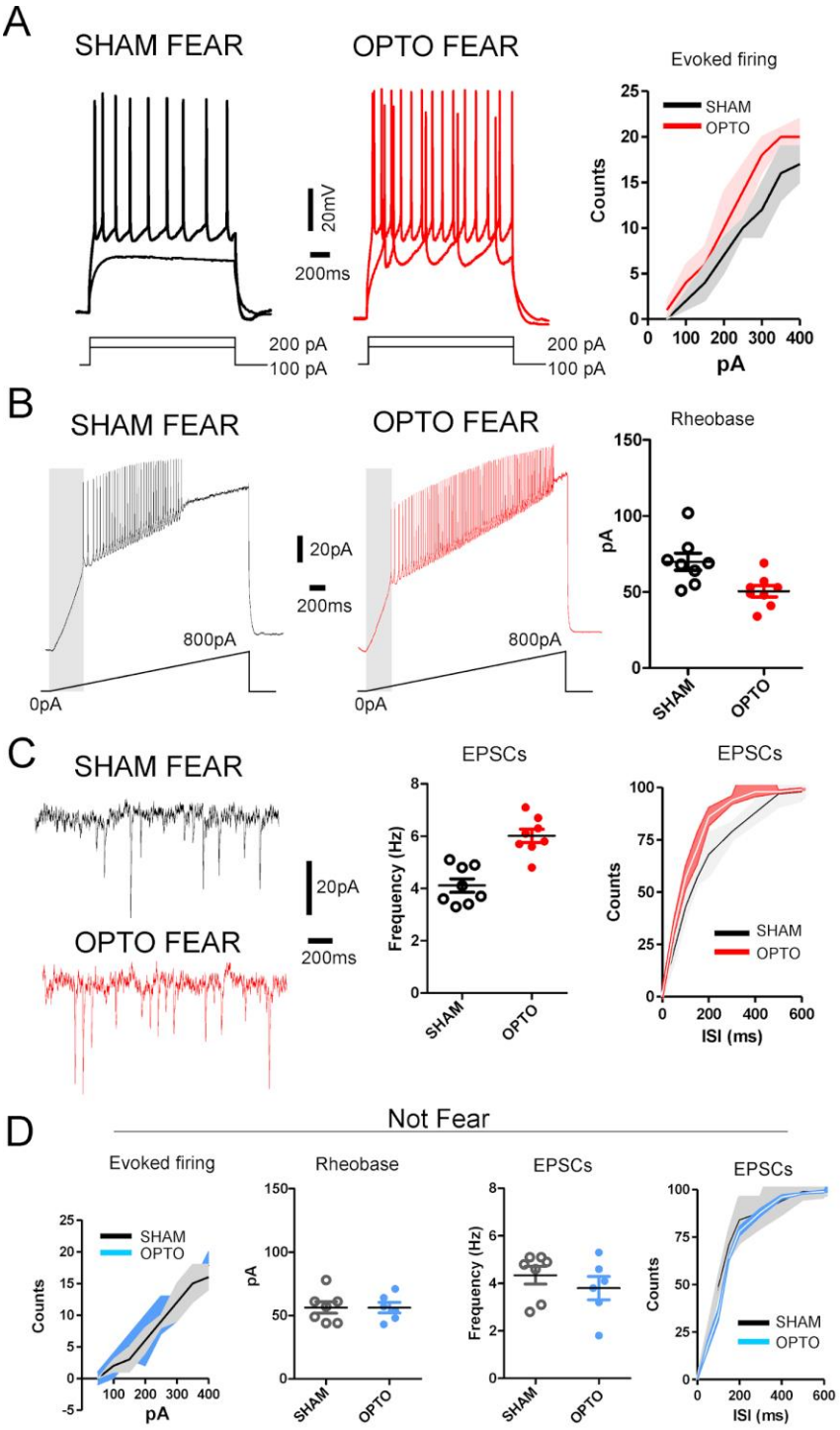

Figure 2. Modulation of cellular excitability of PreLimbic (PrL) pyramidal neurons by optogenetic stimulation. A) Representative traces in current-clamp configuration reporting evoked firing activity triggered by a series of depolarizing current steps (0 to 400 pA) applied to PrL pyramidal

Preprints (www.preprints.org) | NOT PEER-REVIEWED | Posted: 10 December 2020 doi:10.20944/preprints202012.0252.v1

neurons of SHAM FEAR (black) and OPTO FEAR (red) groups. The cumulative plot shows the changes in firing activity. B) Representative traces of PrL pyramidal neurons of SHAM FEAR (black) and OPTO FEAR (red) groups showing the firing activity triggered by linear depolarization from 0 to 800 pA. Graph (on the right) reports the effects of optogenetic stimulation on rheobase value. C) Representative traces of Excitatory Post-Synaptic Currents (EPSC) of PrL pyramidal neurons of SHAM FEAR (black) and OPTO FEAR (red) groups. Graph plot (in the middle) and cumulative curve (on the right) depict the clear increase in firing frequency in PrL pyramidal neurons of optogenetically-stimulated animals. D) Graphs and cumulative curves report no significant differences in cellular excitability in PrL pyramidal neurons of SHAM NOT FEAR (black) and OPTO NOT FEAR (blue) groups.

2.3 Morphological results: spine counting of PrL pyramidal neurons

The four experimental groups exhibited different spine number and density in apical arborizations of PrL pyramidal neurons, as demonstrated by one-way ANOVAs on number ($F_{3,16}$=14.24; P=0.00009) and density ($F_{3,16}$=12.38; P=0.0002) of dendritic spines. Newman-Keuls post-hoc comparisons indicated that OPTO FEAR group had the highest spine number and density in comparison to the remaining groups (at least P=0.0001) that, in turn, exhibited similar spine number and density.

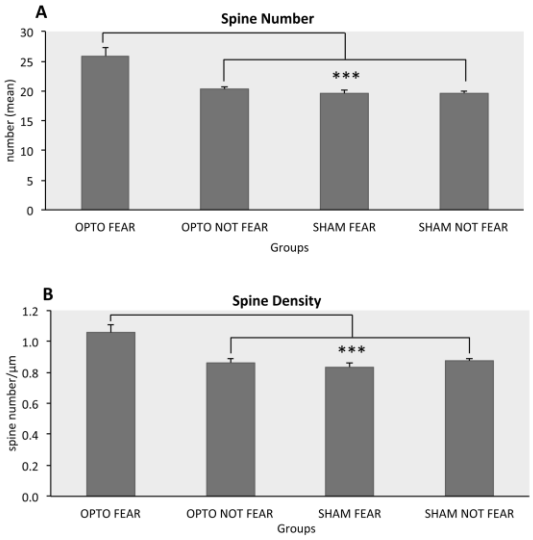

Figure 3. Spine counting of the apical arborizations of PreLimbic pyramidal neurons. OPTO FEAR group had the highest spine number (A) and density (B) in comparison to the remaining groups (*** at least P=0.0001) exhibiting similar spine quantification.

Preprints (www.preprints.org) | NOT PEER-REVIEWED | Posted: 10 December 2020 doi:10.20944/preprints202012.0252.v1

2.4 Transcriptomic results: differential gene expression profiling and functional enrichment analysis of RNA extracted by sorted amygdala pyramidal neurons

Gene expression profiling resulted in 4550 protein-coding genes with a reliable expression and they underwent the downstream analysis. A Principal Component Analysis (PCA) was performed to assess sample clustering based on gene expression profiles (Figure 4). Notably, individual samples belonging to the same group clustered well together. Further, while gene expression profiles of mice belonging to SHAM FEAR and SHAM NOT FEAR groups appeared clustered, those of individuals belonging to OPTO FEAR and OPTO NOT FEAR groups were markedly segregated. Differential expression analysis was performed on 2x2 design (Group x Condition) and Differentially Expressed Genes (DEGs) were identified. Significant differentially expressed genes were identified for a $q>0.95$, equivalent to an FDR-corrected $P<0.05$. Subsequently, Gene Ontology (GO) and Kyoto Encyclopedia of Genes and Genomes (KEGG) annotations and over-representation analyses (ORA) were performed using clusterProfiler (extended results are reported as Supplementary Results 1 and in Supplementary Figure 1). Significant pathways were shown by means of enrichment map method.

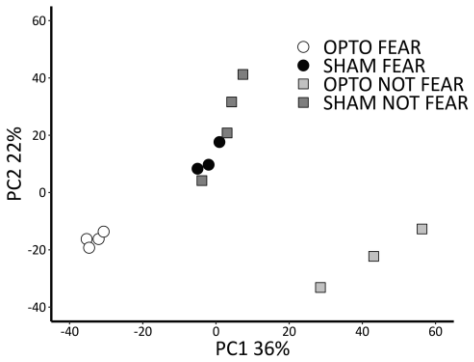

Figure 4. Principal Component Analysis revealing sample clustering based on gene expression profiles. While gene expression profile of mice belonging to SHAM FEAR and SHAM NOT FEAR groups appeared clustered, those of individuals belonging to OPTO FEAR and OPTO NOT FEAR groups were markedly segregated.

2.4.1 Comparison between OPTO FEAR vs. SHAM FEAR groups

Differential Expression analysis showed 2417 significant DEGs (1043 up; 1374 down, with reference level set on the SHAM FEAR condition) (Figure 5A-B, Table 1). To explore further the biological significance of the transcriptomic modulations caused by optogenetic stimulation in

Preprints (www.preprints.org) | NOT PEER-REVIEWED | Posted: 10 December 2020 doi:10.20944/preprints202012.0252.v1

the presence of fear memory, ORA was performed on the obtained DEGs and resulted in 137 significantly enriched GO (Biological Processes, BP: 57; Cellular Component, CC: 61; Molecular Function, MF: 19) terms and 132 significantly enriched KEGG terms. The top twenty significant GO terms belonged to BP and CC and highlighted a differential involvement of the pathways associated with neuronal plasticity and synaptic signaling, resulting in an overall modulation of synaptic organization (Figure 5C) (namely: GO:0098590 Plasma membrane region, GO:0031226 Intrinsic component of plasma membrane, GO:009897 Glutamatergic synapse, GO:0005887 Integral component of plasma membrane, GO:0044456 Synapse part, GO:0030424 Axon, GO:0042734 Presynaptic membrane, GO:0031253 Cell projection membrane, GO:0098794 Postsynapse, GO:0099537 Trans-synaptic signaling, GO:0098609 Cell-cell adhesion, GO:0007155 Cell adhesion, GO:0099536 Synaptic signaling, GO:0022610 Biological adhesion, GO:0007268 Chemical synaptic transmission, GO:0098916 Anterograde trans-synaptic signaling, GO:0030425 Dendrite, GO:0097447 Dendritic tree, GO:0099572 Postsynaptic specialization, and GO:0097060 Synaptic membrane).

The top twenty significant KEGG terms resulted associated to signaling processes related to several neurodegenerative diseases and metabolic pathways (Figure 5D) (namely: mmu05022 Pathways of neurodegeneration - multiple diseases, mmu04144 Endocytosis, mmu05010 Alzheimer Disease, mmu05012 Parkinson Disease, mmu04140 Autophagy – animal, mmu05014 Amyotrophic Lateral Sclerosis, mmu04137 Mitophagy – animal, mmu05132 Salmonella infection, mmu04714 Thermogenesis, mmu04360 Axon guidance, mmu04919 Thyroid hormone signaling pathway, mmu04141 Protein processing in endoplasmic reticulum, mmu05231 Choline metabolism in cancer, mmu04722 Neurotrophin signaling pathway, mmu03010 Ribosome, mmu04072 Phospholipase D signaling pathway, mmu01212 Fatty acid metabolism, mmu01200 Carbon metabolism, mmu05020 Prion disease, and mmu00190 Oxidative phosphorylation).

2.4.2 Comparison between OPTO NOT FEAR vs. SHAM NOT FEAR groups

Differential Expression analysis showed 1661 significant DEGs (308 up; 1353 down, with reference level set on the SHAM NOT FEAR condition) (Figure 5E-F; Table 2). The ORA performed on the obtained DEGs resulted only in 36 significantly enriched KEGG terms and 0 significantly enriched GO terms. Here, the genes universe did not allow enriching many GO terms because of sampling bias correction [38]. Again, the top twenty over-represented KEGG

 doi:10.20944/preprints202012.0252.v1

terms were related to neurodegenerative diseases and metabolic pathways (Figure 5G) (namely: mmu04144 Endocytosis, mmu00190 Oxidative phosphorylation, mmu04140 Autophagy – animal, mmu05014 Amyotrophic Lateral Sclerosis, mmu04714 Thermogenesis, mmu05010 Alzheimer Disease, mmu05012 Parkinson Disease, mmu05022 Pathways of neurodegeneration - multiple diseases, mmu05016 Huntington Disease, mmu01212 Fatty acid metabolism, mmu05020 Prion Disease, mmu04141 Protein processing in endoplasmic reticulum, mmu03040 Spliceosome, mmu04530 Tight junction, mmu04137 Mitophagy – animal, mmu01040 Biosynthesis of unsaturated fatty acids, mmu04932 Non-alcoholic fatty liver disease, mmu04142 Lysosome, mmu01200 Carbon metabolism, and mmu04071 Sphingolipid signaling pathway).

Preprints (www.preprints.org) | NOT PEER-REVIEWED | Posted: 10 December 2020 doi:10.20944/preprints202012.0252.v1

Table 1. The top 20 DEGs identified by differential expression profiling from RNA extracted by amygdala pyramidal neurons Comparison between OPTO FEAR vs. SHAM FEAR groups

Gene symbol	Gene name	Fold change (log2 scale)	OPTO FEAR adj.mean	SHAM FEAR adj.mean
Slc6a17	solute carrier family 6 (neurotransmitter transporter), member 17	-4.24	12.86	242.95
2010300C02Rik	RIKEN cDNA 2010300C02 gene	-4.02	6.95	113.03
Lmo3	LIM domain only 3	-3.80	12.43	172.75
Celf5	CUGBP, Elav-like family member 5	-3.74	12.58	168.18
Hap1	huntingtin-associated protein 1	-3.65	13.22	166.13
Papss2	3'-phosphoadenosine 5'-phosphosulfate synthase 2	-3.60	9.79	118.38
Sphkap	SPHK1 interactor, AKAP domain containing	-3.52	23.12	265.56
Ccdc148	coiled-coil domain containing 148	-3.51	9.18	104.53
Lrp11	low density lipoprotein receptor-related protein 11	-3.50	8.59	97.11
6330403K07Rik	RIKEN cDNA 6330403K07 gene	-3.48	6.08	67.76
Ube2ql1	ubiquitin-conjugating enzyme E2Q family-like 1	-3.47	5.54	61.52
Brinp1	bone morphogenic protein/retinoic acid inducible neural specific 1	-3.47	11.69	129.49
Arpp21	cyclic AMP-regulated phosphoprotein, 21	-3.44	33.80	366.38
Gabra4	gamma-aminobutyric acid (GABA) A receptor, subunit alpha 4	-3.41	12.24	130.15
Csmd1	CUB and Sushi multiple domains 1	-3.39	25.79	269.68
Kcnh3	potassium voltage-gated channel, subfamily H (eag-related), member 3	-3.34	5.02	50.67
Agt	angiotensinogen (serpin peptidase inhibitor, clade A, member 8)	-3.28	33.63	327.00
St6gal2	beta galactoside alpha 2,6 sialyltransferase 2	-3.28	9.03	87.47
Bcl2	B cell leukemia/lymphoma 2	-3.27	17.48	169.00
Cbarp	calcium channel, voltage-dependent, beta subunit associated regulatory protein	-3.23	16.69	156.53

Preprints (www.preprints.org) | NOT PEER-REVIEWED | Posted: 10 December 2020 doi:10.20944/preprints202012.0252.v1

Table 2. The top 20 DEGs identified by differential expression profiling from RNA extracted by amygdala pyramidal neurons Comparison between OPTO NOT FEAR vs. SHAM NOT FEAR groups

Gene symbol	Gene name	Fold change (log2 scale)	OPTO NOT FEAR adj.mean	SHAM NOT FEAR adj.mean
0610010K14Rik	RIKEN cDNA 0610010K14 gene	-4.83	2.44	69.50
Gm10163	predicted pseudogene 10163	-4.15	8.60	153.17
Dipk2a	divergent protein kinase domain 2A	-3.72	34.80	457.61
Nab1	Ngfi-A binding protein 1	-3.61	30.00	366.69
Nkap	NFKB activating protein	-3.56	19.30	227.98
Slc6a9	solute carrier family 6 (neurotransmitter transporter, glycine), member 9	-3.53	67.13	778.02
Agt	angiotensinogen (serpin peptidase inhibitor, clade A, member 8)	-3.51	33.15	378.72
Cpm	carboxypeptidase M	-3.47	45.96	509.16
Ermp1	endoplasmic reticulum metallopeptidase 1	-3.40	61.64	652.31
Gm15500	predicted pseudogene 15500	-3.40	54.43	573.54
Dazap2	DAZ associated protein 2	-3.36	59.16	608.47
Rtl8b	retrotransposon Gag like 8B	-3.35	33.48	340.80
Polm	polymerase (DNA directed), mu	-3.32	6.50	64.73
Gpx4	glutathione peroxidase 4	-3.31	39.34	391.42
Sos1	SOS Ras/Rac guanine nucleotide exchange factor 1	-3.31	73.41	727.62
Ctr9	CTR9 homolog, Paf1/RNA polymerase II complex component	-3.30	67.94	667.74
Tmem184c	transmembrane protein 184C	-3.29	47.58	464.32
Dzank1	double zinc ribbon and ankyrin repeat domains 1	-3.27	36.48	352.91
D430019H16Rik	RIKEN cDNA D430019H16 gene	-3.27	35.99	346.81
Klhl9	kelch-like 9	-3.24	57.35	543.23

Preprints (www.preprints.org) | NOT PEER-REVIEWED | Posted: 10 December 2020 doi:10.20944/preprints202012.0252.v1

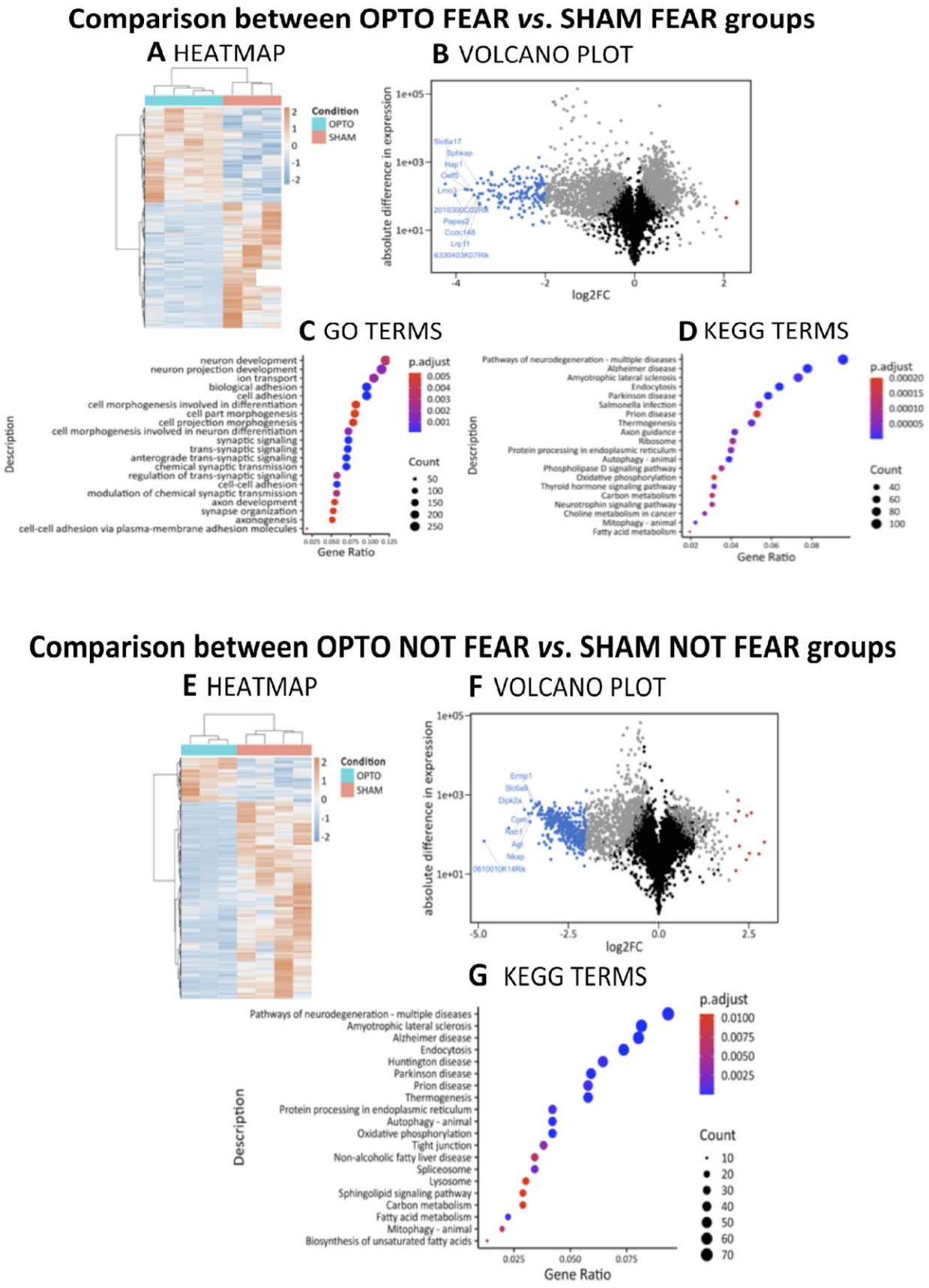

Figure 5. Differential Gene Expression profiling and functional enrichment analysis of RNA extracted by amygdala pyramidal neurons. Comparisons between OPTO FEAR *vs*. SHAM FEAR

groups (upper part) and OPTO NOT FEAR *vs*. SHAM NOT FEAR groups (lower part). A, E) Heatmaps showing gene expression values for the Differentially Expressed Genes (DEGs). B, F) Volcano plots highlighting DEGs. The x-axis is the log2 fold change (log2FC) in normalized gene expression and the y-axis is for the $\log_{10}$ absolute value of the difference in expression between conditions. Each dot represents a gene. Grey dots are for DEGs, blue and red dots are for <-2 and >+2 log2FC genes, respectively. The top ten genes with the highest absolute log2FC values are labeled. C, D, G) Dot plots representing the top twenty enriched terms from over-representation analyses (ORA) in Gene Ontology (GO) and Kyoto Encyclopedia of Genes and Genomes (KEGG) databases. GO terms from different domains (Biological Processes, Cellular Component, and Molecular Function) were sorted by q-value before plotting them together.

2.4.3 Comparison between OPTO FEAR vs. OPTO NOT FEAR groups

Differential Expression analysis showed 3506 significant DEGs (2104 up; 1402 down, with reference level set on the OPTO NOT FEAR condition) (Figure 6A-B, Table 3). Despite the high number of DEGs, the ORA performed on the obtained DEGs resulted only in 3 significantly enriched GO terms (BP: 0; MF: 0; CC: 3, i.e.: GO:0005887 integral component of plasma membrane, GO:0031226 intrinsic component of plasma membrane, and GO:0098590 plasma membrane region), indicating a broad modulation of genes without a significant enrichment for specific pathways. These large differences in transcriptome include crucial pathways linked to neuron morphogenesis and differentiation (e.g., GO:0031175 Neuron projection development, GO:0048667 Cell morphogenesis involved in neuron differentiation, GO:0007409 Axonogenesis, GO:0061564 Axon development, GO:0000904 Cell morphogenesis involved in differentiation) (Supplementary Results).

In parallel, 169 KEGG terms resulted significantly enriched. The top twenty over-represented KEGG terms were associated to neurodegeneration, metabolic regulation, regulation of actin cytoskeleton, and cancer (namely: mmu04144 Endocytosis, mmu05132 Salmonella infection, mmu05022 Pathways of neurodegeneration - multiple diseases, mmu04140 Autophagy – animal, mmu05014 Amyotrophic Lateral Sclerosis, mmu05012 Parkinson Disease, mmu05010 Alzheimer Disease, mmu04530 Tight junction, mmu04137 Mitophagy – animal, mmu04810 Regulation of actin cytoskeleton, mmu05020 Prion disease, mmu04360 Axon guidance, mmu04071 Sphingolipid signaling pathway, mmu05016 Huntington Disease, mmu04141 Protein processing in endoplasmic reticulum, mmu05017 Spinocerebellar ataxia, mmu05211

Preprints (www.preprints.org) | NOT PEER-REVIEWED | Posted: 10 December 2020 doi:10.20944/preprints202012.0252.v1

Renal cell carcinoma, mmu04928 Parathyroid hormone synthesis, secretion and action, mmu01212 Fatty acid metabolism, and mmu04714 Thermogenesis).

2.4.4 Comparison between SHAM FEAR vs. *SHAM NOT FEAR groups*

In line with PCA highlighting poor segregation between SHAM FEAR vs. SHAM NOT FEAR groups, differential Expression analysis showed only 107 significant DEGs (81 up; 26 down, with reference level set on SHAM NOT FEAR condition) (Figure 6D-E, Table 4). Despite the small number of DEGs, the ORA performed on the obtained DEGs resulted in 129 enriched GO terms (BP: 67; CC: 45; MF: 17) and 3 enriched KEGG terms. The top twenty significant GO terms belonged to BP and CC and suggested the differential involvement of pathways related to synaptic plasticity, in particular related to excitatory synapse, and morphogenesis (Figure 6F) (namely: GO:0009986 Cell surface, GO:0048471 Perinuclear region of cytoplasm, GO:0030424 Axon, GO:0036477 Somato-dendritic compartment, GO:0030425 Dendrite, GO:0097447 Dendritic tree, GO:0043025 Neuronal cell body, GO:0098590 Plasma membrane region, GO:0048812 Neuron projection morphogenesis, GO:0048667 Cell morphogenesis involved in neuron differentiation, GO:0120039 Plasma membrane bounded cell projection morphogenesis, GO:0048858 Cell projection morphogenesis, GO:0032279 Asymmetric synapse, GO:0032990 Cell part morphogenesis, GO:0060076 Excitatory synapse, GO:0005887 Integral component of plasma membrane, GO:0098984 Neuron to neuron synapse, GO:0044456 Synapse part, GO:0097038 Perinuclear endoplasmic reticulum, and GO:0033267 Axon part). KEGG analysis showed modulation of the pathways associated to cAMP signaling (mmu04024), Prostate cancer (mmu05215), and Thyroid hormone signaling (mmu04919).

Preprints (www.preprints.org) | NOT PEER-REVIEWED | Posted: 10 December 2020 doi:10.20944/preprints202012.0252.v1

Table 3. The top 20 DEGs identified by differential expression profiling from RNA extracted by amygdala pyramidal neurons Comparison between OPTO FEAR vs. OPTO NOT FEAR groups

Gene symbol	Gene name	Fold change (log2 scale)	OPTO FEAR adj.mean	OPTO NOT FEAR adj.mean
Ube2ql1	ubiquitin-conjugating enzyme E2Q family-like 1	-5.13	5.54	194.27
Slc6a17	solute carrier family 6 (neurotransmitter transporter), member 17	-5.12	12.86	448.21
Papss2	3'-phosphoadenosine 5'-phosphosulfate synthase 2	-4.57	9.79	232.51
Hap1	huntingtin-associated protein 1	-4.29	13.22	258.18
Ngef	neuronal guanine nucleotide exchange factor	-4.28	18.41	358.22
Cpm	carboxypeptidase M	4.24	871.36	45.96
Thy1	thymus cell antigen 1, theta	-4.22	88.57	1649.90
Slc6a9	solute carrier family 6 (neurotransmitter transporter, glycine), member 9	4.16	1202.20	67.13
Arpp21	cyclic AMP-regulated phosphoprotein, 21	-4.15	33.80	599.42
Enc1	ectodermal-neural cortex 1	-4.10	54.26	928.57
Celf5	CUGBP, Elav-like family member 5	-4.08	12.58	212.32
Ermp1	endoplasmic reticulum metallopeptidase 1	4.04	1016.54	61.64
Ptprg	protein tyrosine phosphatase, receptor type, G	-4.04	36.77	603.55
Cxcl14	chemokine (C-X-C motif) ligand 14	-4.02	19.49	315.59
Chrna4	cholinergic receptor, nicotinic, alpha polypeptide 4	-4.01	3.93	63.10
Arsg	arylsulfatase G	4.01	580.93	36.15
Kcnq2	potassium voltage-gated channel, subfamily Q, member 2	-4.00	27.21	436.00
Sfxn1	sideroflexin 1	-3.99	15.50	246.04
Thrb	thyroid hormone receptor beta	-3.91	13.85	208.27
Lmo3	LIM domain only 3	-3.89	12.43	183.70

Preprints (www.preprints.org) | NOT PEER-REVIEWED | Posted: 10 December 2020 doi:10.20944/preprints202012.0252.v1

Table 4. The top 20 DEGs identified by differential expression profiling from RNA extracted by amygdala pyramidal neurons
Comparison between SHAM FEAR vs. SHAM NOT FEAR groups

Gene symbol	Gene name	Fold change (log2 scale)	SHAM FEAR adj.mean	SHAM NOT FEAR adj.mean
Gm13574	predicted gene 13574	-3.48	2.78	30.95
Gm49601	predicted gene, 49601	2.45	17.99	3.30
4931406B18Rik	RIKEN cDNA 4931406B18 gene	-2.31	10.68	52.82
D430019H16Rik	RIKEN cDNA D430019H16 gene	-2.30	23.45	115.51
Sphkap	SPHK1 interactor, AKAP domain containing	-2.25	73.14	346.81
Slx4ip	SLX4 interacting protein	1.98	265.56	67.29
Smcr8	Smith-Magenis syndrome chromosome region, candidate 8 homolog (human)	-1.97	21.56	84.55
Olfr1233	olfactory receptor 1233	1.81	403.22	115.33
Hcn2	hyperpolarization-activated, cyclic nucleotide-gated K+ 2	1.80	27.04	7.74
Sumf1	sulfatase modifying factor 1	1.79	859.93	248.23
Cd99l2	CD99 antigen-like 2	1.60	106.02	34.94
Kif6	kinesin family member 6	1.59	182.58	60.68
Plaa	phospholipase A2, activating protein	1.55	185.44	63.29
Clstn3	calsyntenin 3	1.51	344.56	120.72
Adcyap1r1	adenylate cyclase activating polypeptide 1 receptor 1	1.35	235.84	92.81
Ino80	INO80 complex subunit	-1.28	326.26	789.84
Cpe	carboxypeptidase E	1.27	359.63	148.70
Uty	ubiquitously transcribed tetratricopeptide repeat gene, Y chromosome	-1.23	2559.64	6021.69
Vmn2r114	vomeronasal 2, receptor 114	-1.21	448.82	1040.79
Gm13574	predicted gene 13574	-1.19	720.62	1641.20

Preprints (www.preprints.org) | NOT PEER-REVIEWED | Posted: 10 December 2020 doi:10.20944/preprints202012.0252.v1

Comparison between OPTO FEAR *vs*. OPTO NOT FEAR groups

A HEATMAP

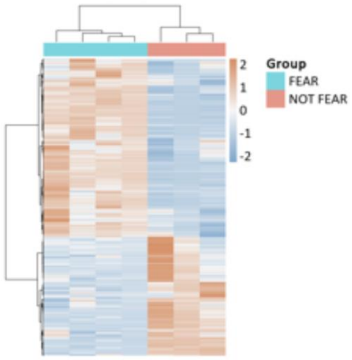

B VOLCANO PLOT

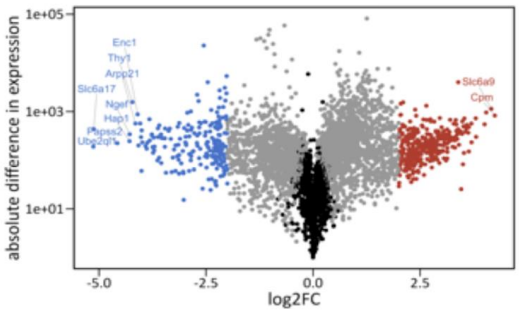

C KEGG TERMS

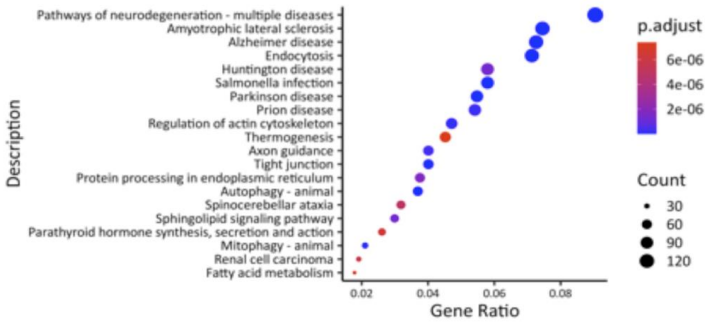

Comparison between SHAM FEAR *vs*. SHAM NOT FEAR groups

D HEATMAP

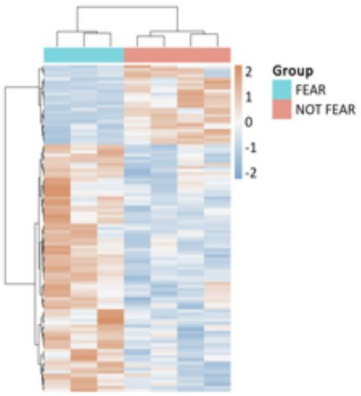

E VOLCANO PLOT

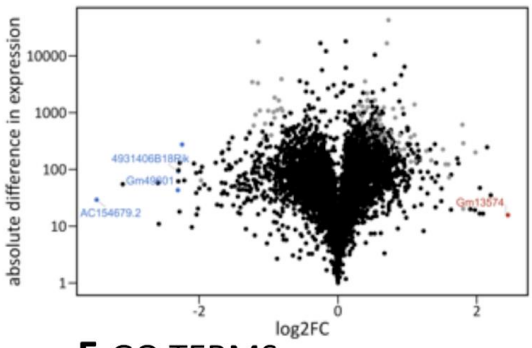

F GO TERMS

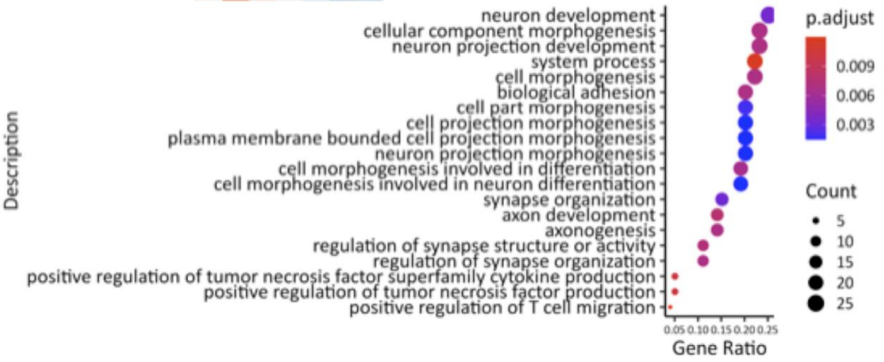

Preprints (www.preprints.org) | NOT PEER-REVIEWED | Posted: 10 December 2020 doi:10.20944/preprints202012.0252.v1

Figure 6. Differential Gene Expression profiling and functional enrichment analysis of RNA extracted by amygdala pyramidal neurons. Comparisons between OPTO FEAR *vs*. OPTO NOT FEAR groups (upper part) and SHAM FEAR *vs*. SHAM NOT FEAR groups (lower part). A, D) Heatmaps showing gene expression values for the Differentially Expressed Genes (DEGs). B, E) Volcano plots highlighting DEGs. The x-axis is the log2 fold change (log2FC) in normalized gene expression and the y-axis is for the $\log_{10}$ absolute value of the difference in expression between conditions. Each dot represents a gene. Grey dots are for DEGs, blue and red dots are for <-2 and >+2 log2FC genes respectively. The top ten genes with the highest absolute log2FC values are labeled. C, F) Dot plots representing the top twenty enriched terms from over-representation analyses (ORA) in Gene Ontology (GO) and Kyoto Encyclopedia of Genes and Genomes (KEGG) databases. GO terms from different domains (Biological Processes, Cellular Component, and Molecular Function) were sorted by q-value before plotting them together.

2.4.5 DEGs involved in learning/memory and fear response in the comparison between OPTO FEAR vs. SHAM FEAR groups

Despite the relative pathways were not identified as significantly enriched, we wondered whether genes involved in learning/memory and fear response were significantly modulated in the case of impaired fear extinction caused by the optogenetic stimulation on PrL pyramidal neurons.

By looking at genes with GO annotations related to BP associated to Learning/memory and Fear response, we identified several DEGs between OPTO FEAR *vs*. SHAM FEAR groups (with reference level set on the SHAM FEAR condition; genes related to Learning/memory: Learning or Memory, 64 over 103 from the gene universe, Learning, 41 over 63, Memory, 25 over 45, Associative Learning, 18 over 23, Long-term memory, 9 over 16, and Visual Learning, 18 over 23; genes related to Fear response: Fear Response and Behavioral Fear Response, 13 over 19) (Figure 7, Supplementary Results 2). This set contains 3 of the top twenty DEGs, all down regulated (with the log2 Fold Change (FC) ranging from -4.24 to -3.23): *Brinp1* (associated to Fear response and Memory), *Bcl2* (associated to Fear response), and *Agt* (associated to Learning) in the comparison between OPTO FEAR and SHAM FEAR groups. We also identified several genes well known to be associated with fear extinction: *ApoE*, *Cacna1* (*Cav1.2*), *Creb1*, *App* and *Arc*. Most of them appeared to be down regulated in the comparison between OPTO FEAR *vs*. SHAM FEAR groups, but to lesser extent (*Apoe* log2FC=-0.33; *Cacna1c* (*Cav1.2*)

Preprints (www.preprints.org) | NOT PEER-REVIEWED | Posted: 10 December 2020 doi:10.20944/preprints202012.0252.v1

log2FC=-0.94; *Creb1* log2FC=-0.96), while we noted a mild but significant increase in the expression of *App* (log2FC=+0.41) and *Arc* (log2FC=0.37) genes. Despite non-being a gene with GO annotations related to BP associated to learning/memory and fear response, we noted that *Homer1*, another gene recently associated to Fear memory extinction, appeared significantly down regulated (log2FC=-0.87), in the comparison between OPTO FEAR *vs*. SHAM FEAR groups. Finally, we also noted the strong down regulation of *Thy1* (log2FC=-2.77) gene.

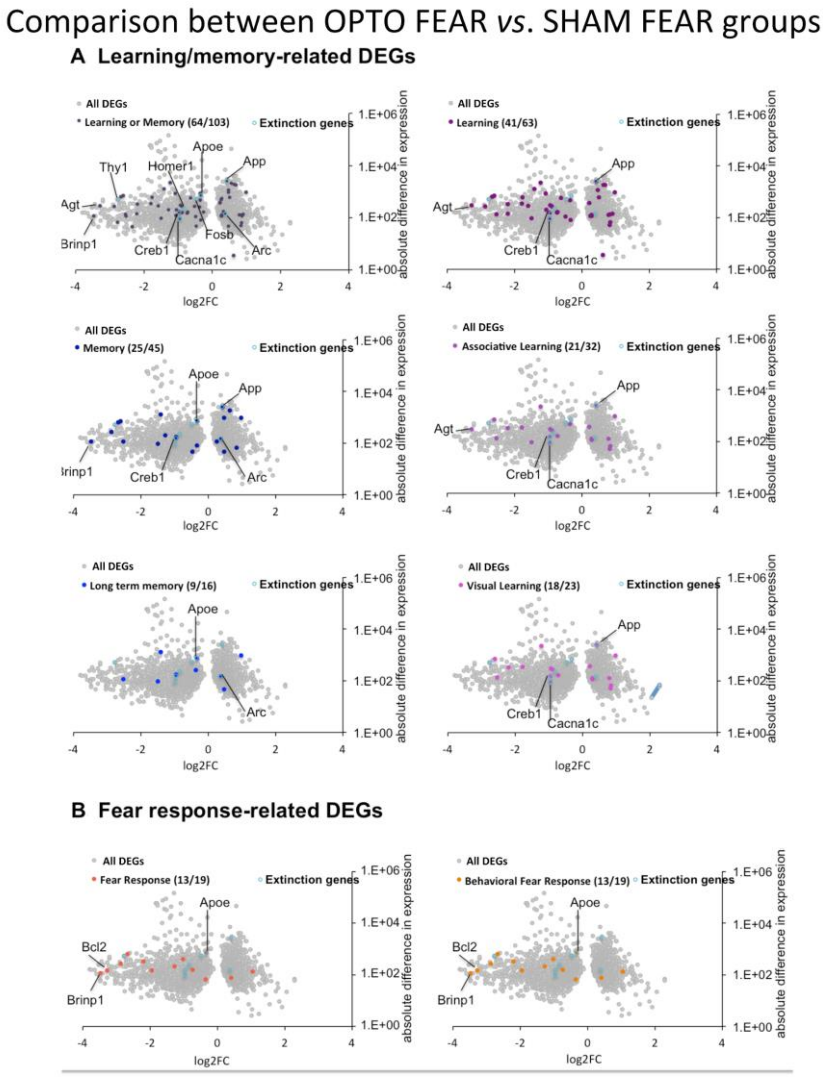

Figure 7: Differentially Expressed Genes (DEGs) with Gene Ontology annotations associated to Learning/memory and Fear response, between OPTO FEAR *vs*. SHAM FEAR groups. DEGs for each indicated Biological Process (BP) are highlighted as colored dots on the volcano plot representing the total DEGs between OPTO FEAR *vs*. SHAM FEAR groups, indicated by grey dots. Numbers into brackets indicate the number of DEGs related to each indicated BP over the gene universe. Light blue dots indicate genes described in literature as associated to fear extinction.

Preprints (www.preprints.org) | NOT PEER-REVIEWED | Posted: 10 December 2020 doi:10.20944/preprints202012.0252.v1

When DEGs are part of the top twenty DEGs list and/or part of the considered BP the gene name is indicated.

3. Discussion

Starting from the assumption that fear learning and extinction are adaptive processes caused by molecular changes in the amygdala-mPFC neural circuit, in the present research adult mice were submitted to CFC receiving (or not) the aversive US as well as the optogenetic (or sham) stimulations to maintain the US-related activation of the PrL pyramidal neurons (receiving from and projecting to the amygdala the fear information) and impair fear extinction. At the end of behavioral testing, cellular excitability and excitatory neurotransmission, as well as spinogenesis, were evaluated in PrL pyramidal neurons. In parallel, amygdala pyramidal neurons were sorted to perform cell-type specific RNA sequencing, able to reveal the specific transcriptional signature of impaired fear extinction.

All fear-conditioned animals (OPTO and SHAM FEAR groups) showed consolidation of aversive memories. However, while SHAM FEAR group progressively extinguished fear memories as expected, no fear extinction was observed in OPTO FEAR group. Thus, the optogenetic activation of PrL pyramidal neurons induced a clear fear extinction deficit. Interestingly, in fear-conditioned mice the optogenetic stimulation induced a robust increase in evoked firing activity, number of action potentials, EPSC frequency, as well as number and density of dendritic spines in the apical arborizations of PrL pyramidal neurons. Conversely, in not fear-conditioned mice the optogenetic stimulation did not produce any significant change in cellular excitability, evoked firing, EPSC frequency, and spinogenesis.

It has been proposed that the boost of amygdala-PrL synaptic transmission leads to changes in the representation of cued fear in mPFC neurons, consistently with enrollment of the amygdala-mPFC network in transmitting the learned CS-US association to the mPFC [19,20]. Optogenetic experiments have confirmed that modified synaptic transmission in the amygdala-PrL network during fear learning interferes with long-term fear consolidation [14]. By using *ex vivo* electrophysiology, combined with optogenetic techniques, it has been demonstrated that fear extinction decreases the efficacy of glutamatergic transmission from mPFC to the amygdala, whereas inhibitory responses are not altered [21]. In parallel, it has been reported that the amygdala neurons projecting to the PrL cortex are active during states of high-fear,

Preprints (www.preprints.org) | NOT PEER-REVIEWED | Posted: 10 December 2020 doi:10.20944/preprints202012.0252.v1

whereas those projecting to IL cortex are recruited and exhibit cell-type-specific plasticity during fear extinction [19].

Cell-type-specific transcriptome analysis represents cutting-edge tool to reveal targets useful for understanding and treating fear-related disorders. Differential gene expression and co-expression network analyses identified diverse networks activated or inhibited by fear learning *vs*. extinction, and upstream regulator analysis and viral vector-manipulations demonstrated that fear extinction is associated with reduced cAMP/Ca^{2+} responsive element binding (CREB) expression [39].

Our study identifies cell-type amygdala pyramidal neuron-specific gene networks (by means of the RNA-sequencing) disclosing pathways mediating adaptive or maladaptive fear extinction and opening innovative possibilities to understand deeper the underlying mechanisms of fear process and its impairment. Here we discuss some of the genes and pathways that result more relevant.

Optogenetic stimulation of the PrL pyramidal neurons resulted in strong modifications of the amygdala pyramidal neuron transcriptome (Figure 5A-B, Table 1). Bioinformatic analyses revealed that among the top twenty DEGs (resulted down regulated in OPTO FEAR mice when compared with SHAM FEAR mice), there were *Gabra4* (Gamma-aminobutyric acid - GABA - A receptor, subunit alpha 4) and *Kcnh3* (potassium voltage-gated channel, subfamily H, member 3), which are associated with synaptic transmission. Namely, shunting inhibition via GABAA receptors reduces activation of N-methyl-D-aspartate receptors, and impairs long-term potentiation [40], as well as voltage-gated potassium channels control cellular excitability by regulating a variety of neuronal properties, such as inter-spike membrane potential, action potential waveform, and firing frequency [41]. Within the brain, *Kcnh3* is expressed in the cerebral cortex, amygdala, hippocampus, and striatal regions, with specific expression in pyramidal neurons [42].

Other DEGs that we identified as associated with impaired extinction were linked to inflammation processes, such as *Csmd1* [43] and *Bcl2* [44]. Notably, overexpression of *Bcl2* blocks the apoptotic death of the pro-B-lymphocyte cells and neurons [45,46]. Furthermore, in the same comparison OPTO FEAR *vs.* SHAM FEAR, the top twenty GO terms associated with impaired extinction highlighted the differential involvement of pathways associated with neuronal plasticity and glutamatergic synaptic signaling, resulting in modulation of overall pre- and post-synaptic organization. In parallel, the top twenty KEGG terms were associated with

 doi:10.20944/preprints202012.0252.v1

processes related to several neurodegenerative diseases, metabolic pathways, production of lipids and proteins, and thyroid hormone and neurotrophin signaling. Remarkably, fear-associated enrichments have been related with dendritic and post-synaptic processes, while extinction-associated enrichments have been related with cellular metabolism and proliferation [39].

By looking at genes related to Learning/memory or Fear response processes, several DEGs were scored in the comparison between OPTO FEAR *vs*. SHAM FEAR groups (Figure 7). Among these, 3 DEGs (i.e., *Brinp1*, associated to Fear response and Memory; *Bcl2*, associated to Fear response; *Agt*, associated to Learning) were part of the most impacted genes (top twenty DEGs), and resulted strongly down regulated in OPTO FEAR group. Several genes previously associated with fear extinction in the literature [39,47–52] were present in OPTO FEAR group, as down regulated (*Apoe, Cacna1c, Creb1, Homer1*) or up regulated (*App, Arc*). Although not always the afore-mentioned genes have been associated specifically to amygdala activity, those down regulated have been positively associated with extinction, while those up regulated have been positively associated with fear memory retention.

The photo-stimulation of PrL pyramidal neurons in the presence or absence of fear differently modulated amygdala pyramidal neuron transcriptome (Figure 6A-B, Table 3). Among the top twenty DEGs, some relevant genes resulted down regulated in OPTO FEAR mice when compared with OPTO NOT FEAR mice. Among these genes, there was *Ngef* (Neuronal guanine nucleotide exchange factor, also known as Ephexin1), an ephrin (Eph) receptor-interacting exchange protein that promotes EphA4 binding and leads to cell morphology changes [53] and reduces spine density [54]. Accordingly, the OPTO FEAR mice (in which *Ngef is down regulated*) exhibited increased number and density of dendritic spines in the apical arborizations. Furthermore, the binding of Eph with its receptors constitutes a molecular link between Eph receptors and actin cytoskeleton and modulates pre-synaptic calcium channel activity [55]. To explore the role of another member of Eph family (EphB2) in memory formation and enhancement, Alapin et al. (2018) used a photo-activatable EphB2 to activate EphB2 forward signaling in pyramidal neurons of the lateral amygdala. Such a photo-activation during fear learning (but not afterwards) enhances the long-term (but not the short-term) fear response. Accordingly, long-term fear memory is impaired in mice lacking EphB2 forward signaling [56].

Among top twenty DEGs, another gene associated with actin-binding protein was *Enc1* (ectodermal-neural cortex 1) that resulted down regulated in OPTO FEAR mice. Kim et al. (1998)

Preprints (www.preprints.org) | NOT PEER-REVIEWED | Posted: 10 December 2020 doi:10.20944/preprints202012.0252.v1

showed that expression of *Enc1* induces neuronal process formation, whereas antisense treatment inhibits neurite development [57]. Similarly, *Thy-1* (thymus cell antigen 1) involved in cell-cell interactions, *Ptprg* (protein tyrosine phosphatase, receptor type, G) implicated in the control of cellular proliferation, and *Kcnq2* (potassium voltage-gated channel, subfamily Q, member 2) were down regulated in OPTO FEAR mice. It has been demonstrated that Kcnq2-related proteins are localized on pyramidal neurons, suggesting their pre-synaptic role in action potential propagation and neurotransmitter release [58]. Even *Chrna4* (cholinergic receptor, nicotinic, alpha polypeptide 4) linked to the superfamily of ligand-gated ion channels that mediate fast signal transmission, was down regulated in OPTO FEAR mice. Of note, as an ancillary remark on the extinction process, mice optogenetically stimulated on amygdala cholinergic input during the initial fear learning are more resistant to extinction learning than controls, supporting the role of cholinergic modulation of amygdala circuits in learning and retention of fear memories [59].

Deficit in exploratory behavior and cognitive impairment in learning tasks as well as neuronal death are reported in mutant mice for *Arsg* gene (arylsulfatase G) [60]. Consistently, our analysis shows *Arsg* down regulation in OPTO FEAR mice. Despite the high number (3506) of DEGs, while only 3 GO terms (components of plasma membrane) were enriched, while 169 KEGG terms resulted enriched. The top twenty over-represented KEGG terms were associated with neurodegeneration, metabolism, actin cytoskeleton regulation, and parathyroid hormone regulation.

Optogenetic stimulation of the PrL pyramidal neurons *per se*, without fear experience, also resulted in a strong modulation of the amygdala transcriptome, and in particular led to down regulation of gene expression (Figure 5E-F; Table 2). Among DEGs (down regulated in OPTO NOT FEAR mice when compared with SHAM NOT FEAR mice), some genes were implicated in cell proliferation, synaptic activation, and long term potentiation (such as *Nab1* and *Sos1*), others in inflammation processes (such as *Gpx4* and *Nkap*), with roles in transcriptional repression and RNA splicing and processing (*Nkap*) [61]. Furthermore, in the same comparison the gene universe did not allow enriching many GO terms because of sampling bias correction [38]. Again, the top twenty over-represented KEGG terms were related to neurodegenerative diseases, metabolic pathways, and biosynthesis of protein and unsaturated fatty acids.

Finally, we observed that fear conditioning *per se*, without optogenetic stimulation, did not greatly impact gene expression in amygdala pyramidal neurons (Figure 6D-E, Table 4), in line

Preprints (www.preprints.org) | NOT PEER-REVIEWED | Posted: 10 December 2020 doi:10.20944/preprints202012.0252.v1

with PCA highlighting poor segregation between SHAM FEAR *vs.* SHAM NOT FEAR groups. This result is in line with those reported by McCullough et al. (2020) who reported a weak separation between the transcriptomes of fear- and not fear-conditioned animals [39]. The authors discussed their findings as result of stress induced translational changes due to the handling of animals and CS exposure. This hypothesis tested in a separate cohort of mice was confirmed, demonstrating that stress-related genes were similarly regulated in both groups. Thus, it is likely that the signature of associative fear learning was obscured by generalized stress-related changes. However, the limited segregation between SHAM FEAR and SHAM NOT FEAR gene profiles might also be caused even by the time point of the transcriptomic analyses. In fact, gene profiling of the SHAM FEAR group was performed once the animals had extinguished the fear memories, and fear response was over, although the fear engram was likely still stored in the amygdala-hippocampus-mPFC circuit [62].

Actually, among DEGs present in the comparison between SHAM FEAR *vs*. SHAM NOT FEAR groups, some genes (such as *Slx4ip* and *Kif6*) were up regulated in SHAM FEAR group and are implicated in DNA/RNA regulation, maintenance and repair [63,64]. Conversely, the *Ino80* gene resulted down regulated in the same comparison. Notably, it has been reported that the deletion of *Ino80* results in defective cellular proliferation and premature entry into cellular senescence, due to activation of the DNA damage response [65]. Furthermore, other genes associated to metabolism (such as the down regulated *Smcr8* and the up regulated *Clstn3*), neurotransmission (such as the up regulated *Hcn2*), and inflammation (such as the up regulated *Sumf1* and *Plaa*) were found differentially expressed in SHAM FEAR group when compared with SHAM NOT FEAR group. Interestingly, also *Adcyap1r1* (adenylate cyclase activating polypeptide 1 receptor 1) resulted up regulated in SHAM FEAR group. The pituitary adenylate cyclase-activating polypeptide is a hormone that stimulates the secretion of growth hormone, adrenocorticotrophic hormone, catecholamines, and insulin, by its interaction with specific receptors. Interestingly, the methylation of *Adcyap1r1* in peripheral blood has been associated with PTSD, and *Adcyap1r1* mRNA is induced by fear learning [66]. Since DNA methylation of regulatory elements usually acts to repress gene transcription, the findings by Ressler et at. (2011) indicating that methylation of *Adcyap1r1* is associated with impaired fear extinction (as typically occurring in PTSD) together with the present ones indicating that the up regulation of this gene is associated with efficient fear extinction converge in highlighting that the system

Preprints (www.preprints.org) | NOT PEER-REVIEWED | Posted: 10 December 2020 doi:10.20944/preprints202012.0252.v1

pituitary adenylate cyclase-activating polypeptide with its receptors might be an important mediator of abnormal fear responses following trauma [66].

In the same comparison (SHAM FEAR *vs*. SHAM NOT FEAR), the top twenty GO terms were related to morphogenesis and synaptic plasticity, with the important specificity of the excitatory synapse. KEGG analysis showed modulation of the pathways associated to cAMP signaling, cancer, and thyroid hormone signaling.

Overall, our results show that the optogenetic activation of PrL pyramidal neurons in fear-conditioned mice does not allow the disengagement of the amygdala-PrL circuit inducing thus fear extinction deficits, reflected in an increase of cellular excitability, excitatory neurotransmission, and spinogenesis of PrL pyramidal neurons, and in strong modifications of the transcriptome of amygdala pyramidal neurons. Such a difference in gene expression profiles was characterized by down regulation of genes associated with synaptic transmission, specifically the inhibitory GABAergic signaling, as well as by differential involvement of pathways associated with neuronal plasticity and glutamatergic signaling.

Our findings demonstrate that impaired extinction is featured by specific changes of transcriptome that validate previous findings [39], and provide targets for future translational research into cell type-specific control of fear extinction, emphasizing the key role of pyramidal neurons belonging to amygdala-mPFC fear matrix. This type of comprehensive cell-type specific analysis produces an important array of targets potentially useful for diagnosis, treatment, and prevention of fear-related disorders.

4. Material and Methods

4.1 Subjects

Male adult (2.5 month-old) B6.Cg-Tg(Thy1-COP4/EYFP)18Gfng/J (Thy1-COP4) (Jackson Laboratories, Maine, USA) mice were used in the present research. These transgenic mice express the light-activated ion channel, Channelrhodopsin-2 (ChR2), fused to Yellow Fluorescent Protein (YFP) under the control of the mouse thymus cell antigen 1 (*Thy1*) promoter. The expression of the transgenic ChR2-YFP fusion protein is detected in pyramidal layer 5 neurons, in the CA1 and CA3 pyramidal neurons of the hippocampus, amygdala pyramidal neurons, cerebellar mossy fibers, neurons in the thalamus, midbrain and brainstem, and the olfactory bulb mitral cells. Transgene-expressing neurons are morphologically and physiologically comparable to non-mutant neurons. The ChR2 functions as a blue light-driven

Preprints (www.preprints.org) | NOT PEER-REVIEWED | Posted: 10 December 2020 doi:10.20944/preprints202012.0252.v1

cation channel that depolarizes the cell and elicits action potentials. Thus, illuminating ChR2-expressing neurons with blue light (~470 nm) leads to rapid and reversible photo-stimulation evoking action potential firing/neural activity.

The animals were group-housed (4 mice/cage) with food (Mucedola, Milan, Italy) and water *ad libitum*, and kept under a 12-h light/dark cycle with the light on at 07:00 h, controlled temperature (22-23°C) and constant humidity (60±5%). All experiments took place during the light phase. All efforts were made to minimize animal suffering and to reduce their number, in accordance with the European Directive (Directive 2010/63/EU) (Authorization n.534/2019 PR). The animals assigned to the same experimental group were never siblings.

4.2 Experimental procedure

Thy1-COP4 mice were unilaterally implanted with a guide cannula on PrL sub-region of right mPFC and then were (or not) fear-conditioned by using the CFC paradigm with the extinction protocol. During the extinction phase of CFC, the mice received optogenetic (OPTO FEAR group, n=10; OPTO NOT FEAR group, n=10) or sham (SHAM FEAR group, n=10; SHAM NOT FEAR group, n=10) stimulations. At the end of the behavioral testing, the animals were sacrificed. Cellular excitability and spine density of Thy1-COP4-expressing PrL pyramidal neurons were analyzed. Furthermore, in the same samples in which PrL pyramidal neurons were electrophysiologically recorded, Thy1-COP4-expressing BLA pyramidal neurons were sorted to purify individual cell-specific RNA for transcriptomic analyses. Transcriptome-wide analyses were carried out by RNA-sequencing, after total RNA ultra-low input library preparation and sequencing in PE75 mode on Illumina platform.

4.3 Stereotaxic surgery and fiber optic implantations

All mice were anesthetized by using Zoletil 100 (tiletamine HCl 50 mg/mL + zolazepam HCl 50 mg/mL; Virbac, Milan, Italy) and Rompun 20 (xylazine 20 mg/mL; Bayer S.p.A, Leverkusen, Germany) dissolved in a volume of saline of 4.1 mg/mL and 1.6 mg/mL, respectively and intraperitoneally injected in a volume of 7.3 mL/kg. Mice were mounted onto a stereotaxic frame (David Kopf Instruments, California, USA) equipped with a mouse adapter and unilaterally implanted with optic fiber (ThorLabs, New Jersey, USA) above the PrL part of the right mPFC (AP: +1.8 mm, ML: +0.25 mm, DV: -2.00 mm). The coordinates from bregma were measured according to the atlas of Franklin and Paxinos (1997) and Mouse Brain Atlases (The

Preprints (www.preprints.org) | NOT PEER-REVIEWED | Posted: 10 December 2020 doi:10.20944/preprints202012.0252.v1

Mouse Brain Library; www.nervenet.org). Ferrule-terminated implanted optical fibers were secured to the skull using dental acrylic.

Mice were allowed to recover from surgery for 1 week before behavioral testing. During the recovery period, they were habituated to handling and connection of the optic fiber with the optogenetic ferrule. Locations of implanted optical fibers were validated using histology in all experimental mice.

4.4 CFC and in vivo optogenetic stimulations of the PrL pyramidal neurons

As previously described [67,68], the CFC was carried out in a soundproof conditioning chamber (50 cm long, 24.5 cm wide, 26.5 cm high) (Ugo Basile, Varese, Italy) made of gray Perspex with a metal grid floor. A video camera placed above the conditioning chamber allowed observing animal behavior. Before the behavioral testing, the mice were handled to connect the optic fiber with the optogenetic ferrule.

As depicted in Figure 1A, on day 1 (Conditioning phase), each mouse was allowed to explore the conditioning chamber for 3 min (Baseline). Afterward, half of the entire sample received three foot-shocks (0.5 mA, 2.0 s, 1 min inter-shock interval), representing the US. The fear-conditioned animals were removed from the conditioning chamber after 1 min from the third foot-shock, while the not fear-conditioned animals were removed after 6 min from the insertion in the chamber, to return to their home cages. The employed foot-shock parameters evoked signs of discomfort as freezing, flinching, jumping, and vocalizing.

On days 2, 3, 4, 7, and 14 (Extinction phase), the fear-conditioned and not fear-conditioned mice were placed again in the conditioning chamber for 6 min. During the Extinction phase, no shock was delivered and the mice received optogenetic or sham stimulation on PrL pyramidal neurons of mPFC, by connecting the optic fiber to a light power source (473 nm; pE2, CoolLED, Andover, UK). Light stimulation parameters were 2s, 20 Hz, 15 ms pulses, 1 pulse every minute of extinction session, density 14.32-15.91 mW/mm^2. No light was delivered on sham-stimulated mice. Notably, *in vivo* optogenetic manipulation of PrL pyramidal neurons was delivered in fear-conditioned mice to reconsolidate and maintain fear memories.

Freezing was recorded by an experimenter blind to the group the animal belonged to and freezing times during the first 3 min for Conditioning (Baseline) and Extinction phases as well as during the entire 6 min for the last day of Extinction phase were compared among groups.

Preprints (www.preprints.org) | NOT PEER-REVIEWED | Posted: 10 December 2020 doi:10.20944/preprints202012.0252.v1

4.5 Slice preparation and electrophysiological recordings of PrL pyramidal neurons

On day 14 of CFC, half of the entire sample of mice (n=5/group) was anesthetized with an overdose of halothane (Sigma-Aldrich, Missouri, USA) and decapitated. Once removed, the brain was attached with cyanoacrylate glue to a tray and then sectioned into 275 µM-thick coronal slices by means of a vibratome (Leica VT1200s, Wetzlar, Germany). During slicing, brain was maintained in ice-cold artificial cerebrospinal fluid solution (ACSF) containing (in mM): NaCl (126), $NaHCO_3$ (26), KCl (2.5), NaH_2PO_4 (1.25), $MgSO_4$ (2), $CaCl_2$ (2) and glucose (10), gassed with 95% O_2–5% CO_2 (pH 7.4, 300 mOsm). Slices were maintained in the same solution at room temperature (~22°C) for at least 30 min. Then, a single slice was transferred to a recording chamber mounted on upright infrared microscopy (BX51WI Olympus, Tokyo, Japan) and continuously perfused with oxygenated ACSF (30°C, 2.5 mL/min) for electrophysiological recordings. Cells were visualized with a 40x water-immersion objective (LumpPlanFI, Olympus, Tokyo, Japan) and by an infrared camera EM-CCD camera (ImagEm, Hamamatsu, Hamamatsu City, Japan). Patch-clamp recordings were made by borosilicate glass pipette (3-5 MΩ) pulled with a micropipette puller (P97, Sutter Instruments, California, USA). For current-clamp experiments, the pipette was filled with a solution containing (in mM): $KMeSO_4$ (140), KCL (10), HEPES (10), Mg_2ATP (2) and Na_3GTP (0.4) (pH adjusted to 7.25 with KOH). For voltage-clamp experiments, the intracellular solution contained (in mM): $CsMeSO_3$ (140), EGTA (1), $CsCl_2$, (5.5), $CaCl_2$ (0.1), HEPES (1), $MgCl_2$ (2) Mg-ATP (2) (pH adjusted to 7.3, 290 mOsm). Electrophysiological recordings were acquired by a Multiclamp 700b amplifier, Digidata 1550A, and pClamp 10.4 software (Molecular Devices, California, USA). Signals were digitized at 10 or 20 kHz and filtered at 2 kHz with a low-pass Bessel filter. For voltage-clamp experiments, series resistance was monitored by repeated 5 mV steps. Cells showing an increase of over 20% in series resistance were discarded from statistical analysis. Spontaneous synaptic events were analyzed off-line by using the Minianalysis Program (Synaptosoft Inc., Georgia, USA) and ClampFit 10.2 (Molecular Devices, California, USA).

4.6 Spine counting of PrL pyramidal neurons

On day 14 of CFC, the remaining half of the entire sample of mice (n=5/group) was anesthetized with an overdose of Zoletil (800 mg/kg; Virbac, Milan, Italy) + Rompun (200 mg/kg; Bayer S.p.A, Leverkusen, Germany) dissolved in a volume of saline of 4.1 mg/mL and 1.6 mg/mL respectively, and intraperitoneally injected. The animals were decapitated, the brains were

Preprints (www.preprints.org) | NOT PEER-REVIEWED | Posted: 10 December 2020 doi:10.20944/preprints202012.0252.v1

rapidly removed, fixed in 4% paraformaldehyde for 24h, and then cryoprotected in 30% sucrose solution. The brains were cut on a freezing microtome into 50 µm-thick coronal sections. Sections were collected at the level of PrL region of mPFC (AP: from 2.68 mm to 1.80 mm from bregma) [69] and then mounted onto slides, dehydrated, and coverslipped using Fluoromount (Sigma-Aldrich, Missouri, USA).

Dendritic spine counts were performed using an optical microscope (Axio Imager M2, Zeiss, Oberkochen, Germany) equipped with a motorized stage and a camera connected to software Neurolucida 2020.1.2 (MicroBright-Field, Vermont, USA). Dendrites were traced with spines and images then exported to Neurolucida™ Explorer 2019.2.1 (MicroBright-Field, Vermont, USA) for spine quantitation.

Due to the difficulty of unequivocally distinguishing filopodia from long thin spines, spine counts included all types of dendritic protrusions ≤4 µm on apical dendrites regardless of their shape or actual function.

Ten dendritic segments (length 20-25 µm) were obtained for each subject of the entire sample (5 animals per group). Spine density was calculated by measuring the length of the dendrite segment and counting the number of spines a long the segment.

4.7 Amygdala pyramidal neuron-specific RNA sequencing

4.7.1 Dissociation of amygdala tissue for fluorescence-activated cell sorting (FACS)

On day 14 of CFC with or without the US, the brains from which PrL pyramidal neurons of mPFC were electrophysiologically recorded were cut to take bilateral amygdala 1-mm punches. Manual and enzymatic dissociations were performed using the Neural Tissue Dissociation Kit (P) (Miltenyi Biotec, Bergisch Gladbach, Germany) with some modifications. Each solution was kept on ice to minimize RNA degradation. Pipette tips were pre-coated in a 0.2 µM filtered 1x PBS-0.5% BSA. Briefly, the amygdala punches were placed on a 35 mm diameter Petri dish, cut into small pieces using a scalpel, and 1 mL of cold Hanks' Balanced Salt Solution without Mg^{2+} and Ca^{2+} (HBBS w/o) (Sigma-Aldrich, Missouri, USA) was added. The tissue was transferred into a 1.5 mL protein LoBind tube. Additional 1 mL HBBS w/o was used to rinse the dish and added to the 1.5 mL tube. Tissue was centrifuged at 300xg for 2 min at room temperature, and the supernatant was carefully aspirated. Then, 975 µL of pre-heated enzyme mix 1 (enzyme P 25 µL, buffer X 950 µL) was added to the tissue, and the 1.5 mL tube was incubated for 15 min at 37°C under slow, continuous rotation using the MACSmix Tube Rotator (Miltenyi Biotec, Bergisch

Preprints (www.preprints.org) | NOT PEER-REVIEWED | Posted: 10 December 2020 doi:10.20944/preprints202012.0252.v1

Gladbach, Germany). Then, 15 µL enzyme mix 2 (enzyme A 5 µL, buffer Y 10 µL) was added to the sample. The sample was gently inverted to mix and mechanically dissociated using the wide-tipped fire-polished Pasteur pipette by pipetting up and down 10 times slowly, followed by a further incubation in the rotator for 10 min at 37°C under slow rotation. The second round of mechanical dissociation was performed using serially fire-polished filtered-glass Pasteur pipettes with gradual diameter diminution, and pipetting slowly up and down 10 times with each pipette, or as long as until tissue pieces were not yet observable. The sample was again incubated at 37°C for 10 min using rotator under slow rotation, before being strained through MACS Smart Strainer (70 µm) (Miltenyi Biotec, Bergisch Gladbach, Germany), placed on a 15 mL tube, pre-coated with 0.2 µM filtered 1x PBS-0.5% BSA, adding 8 mL of HBBS with Mg^{2+} and Ca^{2+}. Then, the cell sample was centrifuged at 300xg for 10 min at room temperature and the supernatant was completely aspirated and collected into a new 15 mL tube, and centrifuged again at 300xg for 10 min at room temperature. The supernatant was again completely aspirated. The pellets obtained from these two centrifugations were pooled into a 1x PBS-0.5% BSA pre-coated SNAP-cap tube containing 1 mL of PBS. Finally, 20U Superase-Inhibitor (Ambion, ThermoFisher, Massachusetts, USA) was added and samples were stored on ice up to sorting.

4.7.2 Cell sorting and isolation of purified pyramidal neurons

For the instrument set-up, samples collected from the amygdala of wild-type YFP-negative mice were used to gate based on forward scatter (FSC) and side scatter (SSC) light scattering and to set the negative (YFP-). Afterward, amygdala samples were collected from the Thy1-COP4 mice and stained with 1 µl of propidium iodide (PI) in order to identify dead cells. Pyramidal neurons were then sorted by using the MoFlo Astrios EQ (Beckman Coulter, California, USA) and the positive cells were collected on the basis of their physical parameters, singlets, PI negative (live cells), and YFP intensity (Figure 8). For initial characterization, samples were collected in PBS and samples examined under a fluorescent microscope to verify correct sorting. Thereafter, cells were sorted directly into ice-cold lysis buffer (Reliaprep RNA Cell Miniprep System, Promega, Wisconsin, USA), mixed by vortexing, kept on ice, and then stored at -80°C until RNA extraction.

Preprints (www.preprints.org) | NOT PEER-REVIEWED | Posted: 10 December 2020 doi:10.20944/preprints202012.0252.v1

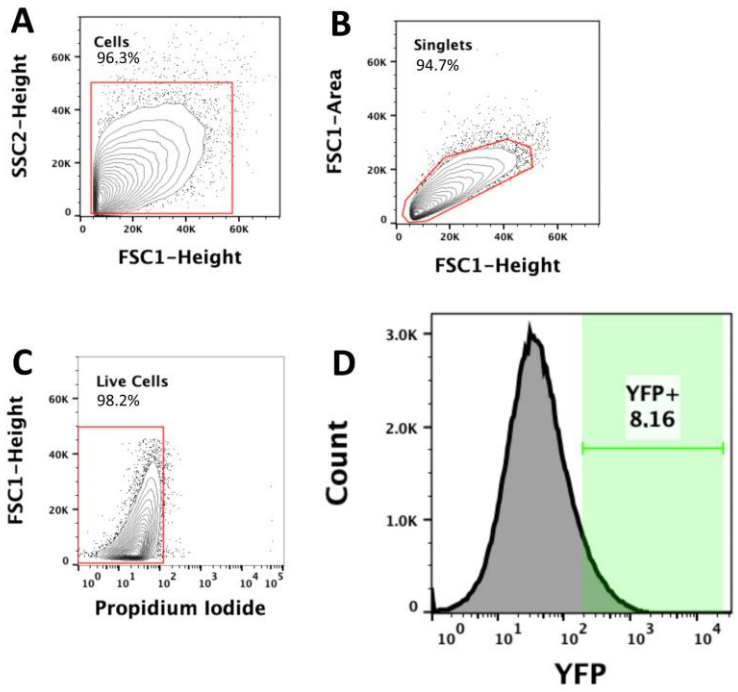

Figure 8. Gating strategy for amygdala pyramidal neurons cell purification. Amygdala pyramidal neurons, excited with a ~488 nm blue laser, were sorted on the basis of their physical parameters (forward scatter, FSC, and side scatter, SSC, light scattering) (A), singlets (B), propidium iodide negative (live cells) (C) and Yellow Fluorescent Protein (YFP) intensity (D), and the positive cells were collected. Cells are sorted by high-speed cell sorting (Moflo Astrios EQ).

4.7.3 RNA-seq library preparation

After thawing on ice in presence of additional proteinase K, RNA was isolated according to manufacturer's instructions including on-column DNase treatment. RNA samples were quantified and the quality tested by Agilent 2100 Bioanalyzer RNA assay (Agilent Technologies, California, USA) or Caliper (PerkinElmer, Massachusetts, USA) (Table 5).

Library preparation and sequencing were performed at IGATechnology (Udine, Italy). At least 3 independent biological replicates were used for each group (Table 5). Each replicate corresponds to the amygdala of a single Thy1-COP4 animal.

Libraries were generated from each sample individually, starting from 0.05-1.4 ng of total RNA, using the Ovation SoLo RNA-seq kit for Ultra-low input (Tecan Genomics, California, USA), following the manufacturer's instructions (library type: fr-second strand). Final libraries were checked with both Qubit 2.0 Fluorometer (Invitrogen, California, USA) and Agilent Bioanalyzer

Preprints (www.preprints.org) | NOT PEER-REVIEWED | Posted: 10 December 2020 doi:10.20944/preprints202012.0252.v1

DNA assay (Agilent Technologies, California, USA) or Caliper (PerkinElmer, Massachusetts, USA). Libraries were then prepared for sequencing and sequenced on paired-end 2x75 bp mode on NextSeq500 (Illumina, California, USA) producing 35.2 MR on average (min 30.4 MR, max 51.7 MR). For the processing of raw data (format conversion and de-multiplexing), Bcl2Fastq 2.20 version of the Illumina pipeline was used. Sequencing data have been deposited in the NCBI Short Read Archive (https://www.ncbi.nlm.nih.gov/geo; GEO accession number GSE162417).

Conditioning	PrL stimulation	Sample name	RNA (ng)	Library (ng)	Reads (M)
FEAR	OPTO	ID_FO1	0.540	0.270	33.954
FEAR	OPTO	ID_FO2	0.846	0.423	38.971
FEAR	OPTO	ID_FO3	0.225	0.112	40.455
FEAR	OPTO	ID_FO4	0.410	0.205	34.162
FEAR	SHAM	ID_FS1	0.140	0.070	34.804
FEAR	SHAM	ID_FS2	2.760	1.380	37.340
FEAR	SHAM	ID_FS3	0.640	0.320	30.547
NOT FEAR	OPTO	ID_NF01	1.770	0.885	30.483
NOT FEAR	OPTO	ID_NF02	0.240	0.120	32.432
NOT FEAR	OPTO	ID_NF03	0.510	0.255	34.756
NOT FEAR	SHAM	ID_NFS1	0.360	0.170	31.432
NOT FEAR	SHAM	ID_NFS2	0.520	0.260	30.438
NOT FEAR	SHAM	ID_NFS3	0.110	0.055	36.824
NOT FEAR	SHAM	ID_NFS4	1.060	0.530	54.741

Table 5: Sketch of RNA samples extracted by amygdala pyramidal YFP neurons and sequenced in PE75 mode. Oy samples used for sequencing, i.e. 14 over 20 total, are reported. Four samples did not pass quality control and were excluded from further analyses.

4.7.4 Analysis of RNA sequencing data

GRCm38.p6 genome was used to map the reads, and transcript abundances were estimated using Salmon v1.2 [70]. To obtain gene-level count matrices the quantification data were imported using tximport [71]. All further analyses based on these count matrices were performed with the free software R v4.0.2, Bioconductor v3.11 [72], and the package NOISeq

Preprints (www.preprints.org) | NOT PEER-REVIEWED | Posted: 10 December 2020 doi:10.20944/preprints202012.0252.v1

v2.31.0 [73]. Differences in RNA composition between samples were corrected by the Trimmed mean of M-values (TMM) normalization [74], and filtered for low counts based on a count per million reads (CPM) criteria. Subsequently, ARSyNseq was used to remove the technical batch effect and NOISeqBIO was used to assess differential gene expression ($q>0.95$, equivalent to FDR-corrected $P<0.05$) [73,75]. GO and KEGG pathway analyses were performed by using ClusterProfiler v3.16.1 [76]. The enrichment map method was used to identify functional modules of mutually overlapping gene sets [76,77].

4.8 Statistical Analysis

As regard the behavioral results, a three-factor ANOVA (stimulation x fear x day) on freezing behavior (measured during 0-3 min of contextual FC) and one-factor ANOVA on freezing behavior (measured during 0-6 min of day 14) were used. Newman-Keuls post-hoc comparisons were applied when permitted.

As regard the morphological results, one-factor ANOVAs on spine number and density were used. Newman-Keuls post-hoc comparisons were applied when permitted.

As regard the electrophysiological results, Pearson r Correlation test (for evoked firing activities and EPSC values) and Mann-Whitney U Test (for rheobase and EPSC values) were used.

As for the behavioral, morphological, and electrophysiological results values of $P=0.05$ were considered statistically significant.

As regard the transcriptomic results, after TMM normalization and low counts filtering, the resulting genes underwent the downstream analysis. Batch effect correction was applied with ARSyN and a PCA was performed to assess sample clustering based on their expression profiles. Differential expression analysis was performed on Group x Condition design and DEGs were identified using NOISeqBIO, a non-parametric analysis for biological replicates. Significant differentially expressed genes were identified for a $q>0.95$, equivalent to an FDR-corrected $P<0.05$. Subsequently, GO and KEGG over-representation analyses were performed and significant pathways were represented by means of enrichment map method to visualize and interpret results.

5. Conclusions

Given the critical role the amygdala-PrL pyramidal neurons played in fear processing, the characterization of the structural, neurophysiological and molecular changes of this neuronal

 doi:10.20944/preprints202012.0252.v1

population leading to adaptive or maladaptive fear extinction may provide valuable insight for the study of, and therapeutic interventions in, fear-related and psychiatric disorders.

 doi:10.20944/preprints202012.0252.v1

Acknowledgments

This work was supported by Italian Ministry of Health (Grant number GR-2018-12365733 to L.D. and S.G.).

Author Contributions

Conceptualization, L.D., S.G., O.V. and P.L.; Methodology, L.D., S.G., G.J., C.S., S.L., D.B.M., C.D., M.A., and P.L.; Software, F.C, T.A., P.A., B.F., P.N.; Validation, all authors; Formal Analysis, L.D., F.C., T.A., P.A., B.F., and P.N.; Investigation, all authors; Resources, L.D. and P.L.; Data Curation, L.D; Writing - Original Draft Preparation, all authors; Writing - Review & Editing, L.D and P.L; Visualization, all authors; Supervision, L.D. and P.L; Project Administration, L.D.; Funding Acquisition, L.D and S.G.

Conflicts of Interest

The authors declare no conflict of interest.

References

1. Maren, S.; Fanselow, M.S. The amygdala and fear conditioning: has the nut been cracked? *Neuron* **1996**, *16*, 237–240.
2. Davis, M. The role of the amygdala in conditioned and unconditioned fear and anxiety. *The amygdala* **2000**, *2*, 213–287.
3. LeDoux, J.E. Emotion circuits in the brain. *Annu. Rev. Neurosci.* **2000**, *23*, 155–184.
4. Fanselow, M.S.; Gale, G.D. The amygdala, fear, and memory. *Ann. N. Y. Acad. Sci.* **2003**, *985*, 125–134.
5. Holmes, A.; Singewald, N. Individual differences in recovery from traumatic fear. *Trends Neurosci.* **2013**, *36*, 23–31.
6. Corcoran, K.A.; Quirk, G.J. Recalling safety: cooperative functions of the ventromedial prefrontal cortex and the hippocampus in extinction. *CNS Spectr.* **2007**, *12*, 200–206.
7. Goshen, I.; Brodsky, M.; Prakash, R.; Wallace, J.; Gradinaru, V.; Ramakrishnan, C.; Deisseroth, K. Dynamics of retrieval strategies for remote memories. *Cell* **2011**, *147*, 678–689.
8. Lacagnina, A.F.; Brockway, E.T.; Crovetti, C.R.; Shue, F.; McCarty, M.J.; Sattler, K.P.; Lim, S.C.; Santos, S.L.; Denny, C.A.; Drew, M.R. Distinct hippocampal engrams control extinction and relapse of fear memory. *Nat. Neurosci.* **2019**, *22*, 753–761.
9. Tovote, P.; Fadok, J.P.; Lüthi, A. Neuronal circuits for fear and anxiety. *Nat. Rev. Neurosci.* **2015**, *16*, 317–331.
10. Trouche, S.; Sasaki, J.M.; Tu, T.; Reijmers, L.G. Fear extinction causes target-specific remodeling of perisomatic inhibitory synapses. *Neuron* **2013**, *80*, 1054–1065.
11. Zhu, H.; Pleil, K.E.; Urban, D.J.; Moy, S.S.; Kash, T.L.; Roth, B.L. Chemogenetic inactivation of ventral hippocampal glutamatergic neurons disrupts consolidation of contextual fear memory. *Neuropsychopharmacology* **2014**, *39*, 1880–1892.
12. Johansen, J.P.; Hamanaka, H.; Monfils, M.H.; Behnia, R.; Deisseroth, K.; Blair, H.T.; LeDoux, J.E. Optical activation of lateral amygdala pyramidal cells instructs associative fear learning. *Proc. Natl. Acad. Sci.* **2010**, *107*, 12692–12697.
13. Tye, K.M.; Prakash, R.; Kim, S.-Y.; Fenno, L.E.; Grosenick, L.; Zarabi, H.; Thompson, K.R.; Gradinaru, V.; Ramakrishnan, C.; Deisseroth, K. Amygdala circuitry mediating reversible and bidirectional control of anxiety. *Nature* **2011**, *471*, 358–362.
14. Klavir, O.; Prigge, M.; Sarel, A.; Paz, R.; Yizhar, O. Manipulating fear associations via optogenetic modulation of amygdala inputs to prefrontal cortex. *Nat. Neurosci.* **2017**, *20*, 836–844.
15. Sierra-Mercado, D.; Padilla-Coreano, N.; Quirk, G.J. Dissociable roles of prelimbic and infralimbic cortices, ventral hippocampus, and basolateral amygdala in the expression and extinction of conditioned fear. *Neuropsychopharmacology* **2011**, *36*, 529–538.
16. Beyeler, A.; Eckhardt, C.A.; Tye, K.M. Deciphering memory function with optogenetics. In *Progress in molecular biology and translational science*; Elsevier, 2014; Vol. 122, pp. 341–390 ISBN 1877-1173.
17. Kim, H.-S.; Cho, H.-Y.; Augustine, G.J.; Han, J.-H. Selective control of fear expression by optogenetic manipulation of infralimbic cortex after extinction. *Neuropsychopharmacology* **2016**, *41*, 1261–1273.
18. Hardt, O.; Nadel, L. Systems consolidation revisited, but not revised: the promise and limits of optogenetics in the study of memory. *Neurosci. Lett.* **2018**, *680*, 54–59.
19. Senn, V.; Wolff, S.B.; Herry, C.; Grenier, F.; Ehrlich, I.; Gründemann, J.; Fadok, J.P.; Müller, C.; Letzkus, J.J.; Lüthi, A. Long-range connectivity defines behavioral specificity of amygdala neurons. *Neuron* **2014**, *81*, 428–437.
20. Sotres-Bayon, F.; Sierra-Mercado, D.; Pardilla-Delgado, E.; Quirk, G.J. Gating of fear in prelimbic cortex by hippocampal and amygdala inputs. *Neuron* **2012**, *76*, 804–812.
21. Cho, J.-H.; Deisseroth, K.; Bolshakov, V.Y. Synaptic encoding of fear extinction in mPFC-amygdala circuits. *Neuron* **2013**, *80*, 1491–1507.
22. Bredy, T.W.; Wu, H.; Crego, C.; Zellhoefer, J.; Sun, Y.E.; Barad, M. Histone modifications around individual BDNF gene promoters in prefrontal cortex are associated with extinction of conditioned fear. *Learn. Mem.* **2007**, *14*, 268–276.

23. Chwang, W.B.; O'Riordan, K.J.; Levenson, J.M.; Sweatt, J.D. ERK/MAPK regulates hippocampal histone phosphorylation following contextual fear conditioning. *Learn. Mem.* **2006**, *13*, 322–328.
24. Miller, C.A.; Sweatt, J.D. Covalent modification of DNA regulates memory formation. *Neuron* **2007**, *53*, 857–869.
25. Itzhak, Y.; Anderson, K.L.; Kelley, J.B.; Petkov, M. Histone acetylation rescues contextual fear conditioning in nNOS KO mice and accelerates extinction of cued fear conditioning in wild type mice. *Neurobiol. Learn. Mem.* **2012**, *97*, 409–417.
26. Monsey, M.S.; Ota, K.T.; Akingbade, I.F.; Hong, E.S.; Schafe, G.E. Epigenetic alterations are critical for fear memory consolidation and synaptic plasticity in the lateral amygdala. *PloS One* **2011**, *6*, e19958.
27. Stafford, J.M.; Raybuck, J.D.; Ryabinin, A.E.; Lattal, K.M. Increasing histone acetylation in the hippocampus-infralimbic network enhances fear extinction. *Biol. Psychiatry* **2012**, *72*, 25–33.
28. Duke, C.G.; Kennedy, A.J.; Gavin, C.F.; Day, J.J.; Sweatt, J.D. Experience-dependent epigenomic reorganization in the hippocampus. *Learn. Mem.* **2017**, *24*, 278–288, doi:10.1101/lm.045112.117.
29. Gelernter, J.; Sun, N.; Polimanti, R.; Pietrzak, R.; Levey, D.F.; Bryois, J.; Lu, Q.; Hu, Y.; Li, B.; Radhakrishnan, K. Genome-wide association study of post-traumatic stress disorder reexperiencing symptoms in> 165,000 US veterans. *Nat. Neurosci.* **2019**, *22*, 1394–1401.
30. Halder, R.; Hennion, M.; Vidal, R.O.; Shomroni, O.; Rahman, R.-U.; Rajput, A.; Centeno, T.P.; Van Bebber, F.; Capece, V.; Vizcaino, J.C.G. DNA methylation changes in plasticity genes accompany the formation and maintenance of memory. *Nat. Neurosci.* **2016**, *19*, 102–110.
31. Ryan, T.J.; Roy, D.S.; Pignatelli, M.; Arons, A.; Tonegawa, S. Engram cells retain memory under retrograde amnesia. *Science* **2015**, *348*, 1007–1013.
32. Yehuda, R.; LeDoux, J. Response Variation following Trauma: A Translational Neuroscience Approach to Understanding PTSD. *Neuron* **2007**, *56*, 19–32, doi:10.1016/j.neuron.2007.09.006.
33. Binder, E.B.; Bradley, R.G.; Liu, W.; Epstein, M.P.; Deveau, T.C.; Mercer, K.B.; Tang, Y.; Gillespie, C.F.; Heim, C.M.; Nemeroff, C.B. Association of FKBP5 polymorphisms and childhood abuse with risk of posttraumatic stress disorder symptoms in adults. *Jama* **2008**, *299*, 1291–1305.
34. Champagne, F.A. Epigenetic mechanisms and the transgenerational effects of maternal care. *Front. Neuroendocrinol.* **2008**, *29*, 386–397.
35. Franklin, T.B.; Russig, H.; Weiss, I.C.; Gräff, J.; Linder, N.; Michalon, A.; Vizi, S.; Mansuy, I.M. Epigenetic transmission of the impact of early stress across generations. *Biol. Psychiatry* **2010**, *68*, 408–415.
36. Koenen, K.C.; Uddin, M. FKBP5 polymorphisms modify the effects of childhood trauma. *Neuropsychopharmacology* **2010**, *35*, 1623–1624.
37. Yehuda, R.; Bierer, L.M. The relevance of epigenetics to PTSD: Implications for the DSM-V. *J. Trauma. Stress* **2009**, *22*, 427–434.
38. Timmons, J.A.; Szkop, K.J.; Gallagher, I.J. Multiple sources of bias confound functional enrichment analysis of global-omics data. *Genome Biol.* **2015**, *16*, 1–3.
39. McCullough, K.M.; Chatzinakos, C.; Hartmann, J.; Missig, G.; Neve, R.L.; Fenster, R.J.; Carlezon, W.A.; Daskalakis, N.P.; Ressler, K.J. Genome-wide translational profiling of amygdala Crh-expressing neurons reveals role for CREB in fear extinction learning. *Nat. Commun.* **2020**, *11*, 1–11.
40. Shen, H.; Sabaliauskas, N.; Sherpa, A.; Fenton, A.A.; Stelzer, A.; Aoki, C.; Smith, S.S. A critical role for α4βδ GABAA receptors in shaping learning deficits at puberty in mice. *Science* **2010**, *327*, 1515–1518.
41. Johnston, J.; Forsythe, I.D.; Kopp-Scheinpflug, C. SYMPOSIUM REVIEW: Going native: voltage-gated potassium channels controlling neuronal excitability. *J. Physiol.* **2010**, *588*, 3187–3200.
42. Miyake, A.; Mochizuki, S.; Yokoi, H.; Kohda, M.; Furuichi, K. New ether-à-go-go K(+) channel family members localized in human telencephalon. *J. Biol. Chem.* **1999**, *274*, 25018–25025, doi:10.1074/jbc.274.35.25018.
43. Kraus, D.M.; Elliott, G.S.; Chute, H.; Horan, T.; Pfenninger, K.H.; Sanford, S.D.; Foster, S.; Scully,

S.; Welcher, A.A.; Holers, V.M. CSMD1 is a novel multiple domain complement-regulatory protein highly expressed in the central nervous system and epithelial tissues. *J. Immunol.* **2006**, *176*, 4419–4430.
44. Sentman, C.L.; Shutter, J.R.; Hockenbery, D.; Kanagawa, O.; Korsmeyer, S.J. bcl-2 inhibits multiple forms of apoptosis but not negative selection in thymocytes. *Cell* **1991**, *67*, 879–888, doi:10.1016/0092-8674(91)90361-2.
45. Williams, G.T. Programmed cell death: apoptosis and oncogenesis. *Cell* **1991**, *65*, 1097–1098, doi:10.1016/0092-8674(91)90002-g.
46. Farlie, P.G.; Dringen, R.; Rees, S.M.; Kannourakis, G.; Bernard, O. bcl-2 transgene expression can protect neurons against developmental and induced cell death. *Proc. Natl. Acad. Sci. U. S. A.* **1995**, *92*, 4397–4401, doi:10.1073/pnas.92.10.4397.
47. Clifton, N.E.; Cameron, D.; Trent, S.; Sykes, L.H.; Thomas, K.L.; Hall, J. Hippocampal regulation of postsynaptic density Homer1 by associative learning. *Neural Plast.* **2017**, *2017*.
48. Olsen, R.H.; Agam, M.; Davis, M.J.; Raber, J. ApoE isoform-dependent deficits in extinction of contextual fear conditioning. *Genes Brain Behav.* **2012**, *11*, 806–812.
49. Pardon, M.-C.; Sarmad, S.; Rattray, I.; Bates, T.E.; Scullion, G.A.; Marsden, C.A.; Barrett, D.A.; Lowe, J.; Kendall, D.A. Repeated novel cage exposure-induced improvement of early Alzheimer's-like cognitive and amyloid changes in TASTPM mice is unrelated to changes in brain endocannabinoids levels. *Neurobiol. Aging* **2009**, *30*, 1099–1113, doi:10.1016/j.neurobiolaging.2007.10.002.
50. Rattray, I.; Scullion, G.A.; Soulby, A.; Kendall, D.A.; Pardon, M.-C. The occurrence of a deficit in contextual fear extinction in adult amyloid-over-expressing TASTPM mice is independent of the strength of conditioning but can be prevented by mild novel cage stress. *Behav. Brain Res.* **2009**, *200*, 83–90.
51. Temme, S.J.; Murphy, G.G. The L-type voltage-gated calcium channel CaV1.2 mediates fear extinction and modulates synaptic tone in the lateral amygdala. *Learn. Mem. Cold Spring Harb. N* **2017**, *24*, 580–588, doi:10.1101/lm.045773.117.
52. Trent, S.; Barnes, P.; Hall, J.; Thomas, K.L. AMPA receptors control fear extinction through an Arc-dependent mechanism. *Learn. Mem. Cold Spring Harb. N* **2017**, *24*, 375–380, doi:10.1101/lm.045013.117.
53. Shamah, S.M.; Lin, M.Z.; Goldberg, J.L.; Estrach, S.; Sahin, M.; Hu, L.; Bazalakova, M.; Neve, R.L.; Corfas, G.; Debant, A.; et al. EphA receptors regulate growth cone dynamics through the novel guanine nucleotide exchange factor ephexin. *Cell* **2001**, *105*, 233–244, doi:10.1016/s0092-8674(01)00314-2.
54. Fu, W.-Y.; Chen, Y.; Sahin, M.; Zhao, X.-S.; Shi, L.; Bikoff, J.B.; Lai, K.-O.; Yung, W.-H.; Fu, A.K.; Greenberg, M.E. Cdk5 regulates EphA4-mediated dendritic spine retraction through an ephexin1-dependent mechanism. *Nat. Neurosci.* **2007**, *10*, 67–76.
55. Frank, C.A.; Pielage, J.; Davis, G.W. A presynaptic homeostatic signaling system composed of the Eph receptor, ephexin, Cdc42, and CaV2.1 calcium channels. *Neuron* **2009**, *61*, 556–569, doi:10.1016/j.neuron.2008.12.028.
56. Alapin, J.M.; Dines, M.; Vassiliev, M.; Tamir, T.; Ram, A.; Locke, C.; Yu, J.; Lamprecht, R. Activation of EphB2 forward signaling enhances memory consolidation. *Cell Rep.* **2018**, *23*, 2014–2025.
57. Kim, T.A.; Lim, J.; Ota, S.; Raja, S.; Rogers, R.; Rivnay, B.; Avraham, H.; Avraham, S. NRP/B, a novel nuclear matrix protein, associates with p110(RB) and is involved in neuronal differentiation. *J. Cell Biol.* **1998**, *141*, 553–566, doi:10.1083/jcb.141.3.553.
58. Cooper, E.C.; Aldape, K.D.; Abosch, A.; Barbaro, N.M.; Berger, M.S.; Peacock, W.S.; Jan, Y.N.; Jan, L.Y. Colocalization and coassembly of two human brain M-type potassium channel subunits that are mutated in epilepsy. *Proc. Natl. Acad. Sci. U. S. A.* **2000**, *97*, 4914–4919, doi:10.1073/pnas.090092797.
59. Jiang, L.; Kundu, S.; Lederman, J.D.; López-Hernández, G.Y.; Ballinger, E.C.; Wang, S.; Talmage, D.A.; Role, L.W. Cholinergic signaling controls conditioned fear behaviors and enhances plasticity of cortical-amygdala circuits. *Neuron* **2016**, *90*, 1057–1070.
60. Kowalewski, B.; Lamanna, W.C.; Lawrence, R.; Damme, M.; Stroobants, S.; Padva, M.; Kalus, I.;

Frese, M.-A.; Lübke, T.; Lüllmann-Rauch, R.; et al. Arylsulfatase G inactivation causes loss of heparan sulfate 3-O-sulfatase activity and mucopolysaccharidosis in mice. *Proc. Natl. Acad. Sci. U. S. A.* **2012**, *109*, 10310–10315, doi:10.1073/pnas.1202071109.

61. Burgute, B.D.; Peche, V.S.; Steckelberg, A.-L.; Glöckner, G.; Gaßen, B.; Gehring, N.H.; Noegel, A.A. NKAP is a novel RS-related protein that interacts with RNA and RNA binding proteins. *Nucleic Acids Res.* **2014**, *42*, 3177–3193, doi:10.1093/nar/gkt1311.
62. Bocchio, M.; Nabavi, S.; Capogna, M. Synaptic Plasticity, Engrams, and Network Oscillations in Amygdala Circuits for Storage and Retrieval of Emotional Memories. *Neuron* **2017**, *94*, 731–743, doi:10.1016/j.neuron.2017.03.022.
63. Li, Y.; Iakoubova, O.A.; Shiffman, D.; Devlin, J.J.; Forrester, J.S.; Superko, H.R. KIF6 polymorphism as a predictor of risk of coronary events and of clinical event reduction by statin therapy. *Am. J. Cardiol.* **2010**, *106*, 994–998, doi:10.1016/j.amjcard.2010.05.033.
64. Svendsen, J.M.; Smogorzewska, A.; Sowa, M.E.; O'Connell, B.C.; Gygi, S.P.; Elledge, S.J.; Harper, J.W. Mammalian BTBD12/SLX4 assembles a Holliday junction resolvase and is required for DNA repair. *Cell* **2009**, *138*, 63–77, doi:10.1016/j.cell.2009.06.030.
65. Min, J.-N.; Tian, Y.; Xiao, Y.; Wu, L.; Li, L.; Chang, S. The mINO80 chromatin remodeling complex is required for efficient telomere replication and maintenance of genome stability. *Cell Res.* **2013**, *23*, 1396–1413.
66. Ressler, K.J.; Mercer, K.B.; Bradley, B.; Jovanovic, T.; Mahan, A.; Kerley, K.; Norrholm, S.D.; Kilaru, V.; Smith, A.K.; Myers, A.J.; et al. Post-traumatic stress disorder is associated with PACAP and the PAC1 receptor. *Nature* **2011**, *470*, 492–497, doi:10.1038/nature09856.
67. Laricchiuta, D.; Centonze, D.; Petrosini, L. Effects of endocannabinoid and endovanilloid systems on aversive memory extinction. *Behav. Brain Res.* **2013**, *256*, 101–107.
68. Laricchiuta, D.; Saba, L.; De Bartolo, P.; Caioli, S.; Zona, C.; Petrosini, L. Maintenance of aversive memories shown by fear extinction-impaired phenotypes is associated with increased activity in the amygdaloid-prefrontal circuit. *Sci. Rep.* **2016**, *6*, 21205, doi:10.1038/srep21205.
69. Franklin, K.B.J.; Paxinos, G. The mouse brain in stereotaxic coordinates Academic Press. *San Diego* **1997**, 186.
70. Patro, R.; Duggal, G.; Love, M.I.; Irizarry, R.A.; Kingsford, C. *Salmon provides fast and bias-aware quantification of transcript expression. Nat Meth. 2017; 14 (4): 417–9*;
71. Soneson, C.; Love, M.I.; Robinson, M.D. *Differential analyses for RNA-seq: transcript-level estimates improve gene-level inferences. F1000Res 4: 1521*; 2015;
72. Gentleman, R.C.; Carey, V.J.; Bates, D.M.; Bolstad, B.; Dettling, M.; Dudoit, S.; Ellis, B.; Gautier, L.; Ge, Y.; Gentry, J. Bioconductor: open software development for computational biology and bioinformatics. *Genome Biol.* **2004**, *5*, R80.
73. Tarazona, S.; Furió-Tarí, P.; Turrà, D.; Pietro, A.D.; Nueda, M.J.; Ferrer, A.; Conesa, A. Data quality aware analysis of differential expression in RNA-seq with NOISeq R/Bioc package. *Nucleic Acids Res.* **2015**, *43*, e140–e140.
74. Robinson, M.D.; Oshlack, A. A scaling normalization method for differential expression analysis of RNA-seq data. *Genome Biol.* **2010**, *11*, 1–9.
75. Nueda, M.J.; Ferrer, A.; Conesa, A. ARSyN: a method for the identification and removal of systematic noise in multifactorial time course microarray experiments. *Biostatistics* **2012**, *13*, 553–566.
76. Yu, G.; Wang, L.-G.; Han, Y.; He, Q.-Y. clusterProfiler: an R Package for Comparing Biological Themes Among Gene Clusters. *OMICS J. Integr. Biol.* **2012**, *16*, 284–287, doi:10.1089/omi.2011.0118.
77. Merico, D.; Isserlin, R.; Stueker, O.; Emili, A.; Bader, G.D. Enrichment map: a network-based method for gene-set enrichment visualization and interpretation. *PloS One* **2010**, *5*, e13984.